NASA TECHNICAL NOTE

NASA TN D-3993

C.1

NASA TN D-3993

TEMPORAL VARIATIONS OF MESOSPHERIC OXYGEN AND OZONE DURING AURORAL EVENTS

by Kaichi Maeda and A. C. Aikin

Goddard Space Flight Center
Greenbelt, Md.

NATIONAL AERONAUTICS AND SPACE ADMINISTRATION • WASHINGTON, D. C. • NOVEMBER 1967

NASA TN D-3993

TEMPORAL VARIATIONS OF MESOSPHERIC OXYGEN AND OZONE DURING AURORAL EVENTS

By Kaîchi Maeda and A. C. Aikin

Goddard Space Flight Center
Greenbelt, Md.

NATIONAL AERONAUTICS AND SPACE ADMINISTRATION

For sale by the Clearinghouse for Federal Scientific and Technical Information
Springfield, Virginia 22151 – CFSTI price $3.00

ABSTRACT

Temporal solutions are given for the photochemical equations describing the distribution of ozone and atomic oxygen in an oxygen atmosphere for the equatorial and polar regions. Similar calculations are applied to auroral events. These calculations indicate a strong dependence of the distribution of mesospheric atomic oxygen on the intensity and energy spectrum of auroral electrons, which dissociate molecular oxygen. It is shown that there can be no significant atmospheric ozone and atomic oxygen modifications due to soft spectrum electron events which appear to characterize most bright auroras. The hard spectrum auroral electrons which appear in most weak, quiet auroras should cause significant increases in the atomic oxygen and ozone concentrations below 80 km, provided that their flux is more than 10^6 per cm^2 sec.

CONTENTS

TEMPORAL VARIATIONS OF MESOSPHERIC OXYGEN AND OZONE DURING AURORAL EVENTS

by
Kaichi Maeda and A. C. Aikin
Goddard Space Flight Center

INTRODUCTION

The dissociation of molecular oxygen by ultraviolet radiation and charged particles, and the subsequent reaction of atomic oxygen with molecular oxygen to form ozone in the earth's atmosphere was first considered by Chapman (1930). Since then, the chemical equations describing the distribution of ozone and atomic oxygen in the mesosphere have been considered by numerous investigators including Bates and Nicolet (1950), Dütsch (1961), Barth (1961), Wallace (1962), Hesstvedt (1963), Leovy (1964) and Hunt (1964; 1965; 1966 a,b). None of these treatments has considered the effect of auroral electrons as a source of molecular dissociation in addition to solar radiation.

Maeda (1962, 1963) has made use of laboratory experiments on the dissociation of oxygen by electron impact (Glockler and Wilson, 1932; Massey and Burhop, 1956) to estimate the dissociation rate of molecular oxygen due to auroral electrons and protons. However, more accurate estimates of the electron impact dissociation cross section as a function of electron energy have been reported recently (Lassettre, Silverman, and Krasnow, 1964; Silverman and Lassettre, 1964; and Bauer and Bartky, 1965).

The new data on O_2-dissociation by electron impact are employed herein to reevaluate the rate coefficient for dissociation by auroral electrons. Also, more rigorous computations are made of electron diffusion in the upper atmosphere in which energy loss, coulomb scattering, and the effects of straggling are taken into account simultaneously (Maeda, 1965 a,b). The resulting rate coefficients are then applied to the calculation of the temporal variation of ozone and atomic oxygen in the mesosphere during auroral events. The calculation is accomplished by solving the time-dependent photochemical equations for a pure oxygen atmosphere in the 50- to 120-km region.

The modification of the ionosphere due to the change in concentration of O and O_3 during charged particle bombardment is discussed, and the effects of diffusion are presented in Appendix A.

DISSOCIATION OF OXYGEN MOLECULES BY ELECTRON IMPACT

Figures 1 and 2 illustrate the potential energy curves for molecular oxygen and the energy level diagram of atomic oxygen, respectively. Excitation of the molecule to repulsive energy levels eventually will lead to the dissociation of the molecule, for which the minimum energy is 5.08 ev. Photon absorption cross sections in the Schumann-Runge continuum have been measured accurately by Watanabe, et al., (1953) and by Ditchburn and Young (1962). Recently, cross sections have been determined accurately for dissociation of oxygen by electron impact.

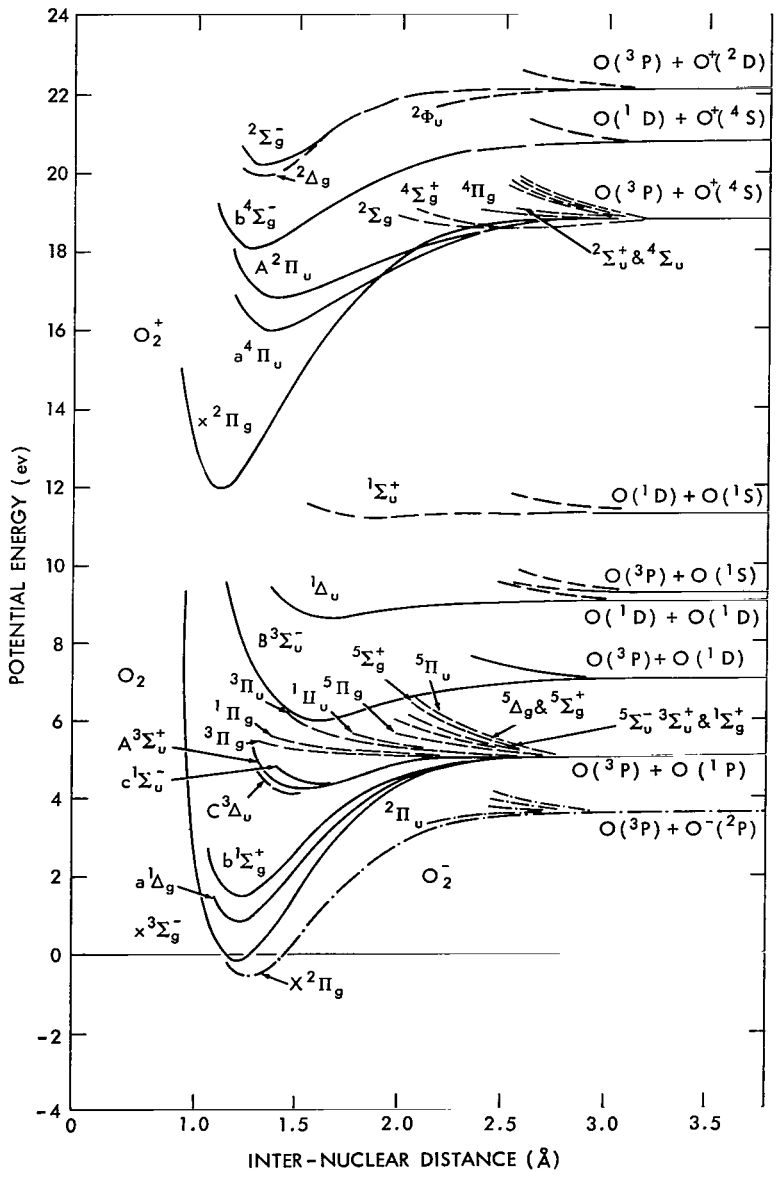

Figure 1—Potential energy curves of molecular oxygen.

Dissociative reactions of oxygen by electron impact can be categorized as follows:

$$O_2 + e \rightarrow O + O^- , \qquad (1)$$

$$\rightarrow O + O^* + e , \qquad (2)$$

and

$$\left.\begin{matrix} O + O^+ + 2e \\ \rightarrow O^- + O^+ + e \\ O^+ + O^+ + 3e \end{matrix}\right\} . \qquad (3)$$

Reaction 1 is the resonance capture of an electron or the so-called resonance dissociative attachment, with the major peak occurring at 6.5 ev (Massey, 1950). The total cross section for dissociative attachment, based on recent measurements by Rapp and Briglia (1964) and Rapp, Sharp and Briglia (1964), is given in Figure 3. At 6.5 ev the maximum cross section for this reaction is 1.5×10^{-18} cm^2. Reaction 2, the dissociation of O_2 into two neutral atoms, is of most interest. The inelastic scattering of electrons with incident energies of 4.5 to 12.5 ev has been studied by Schulz and Dowell (1962), and the results are presented in Figure 4.

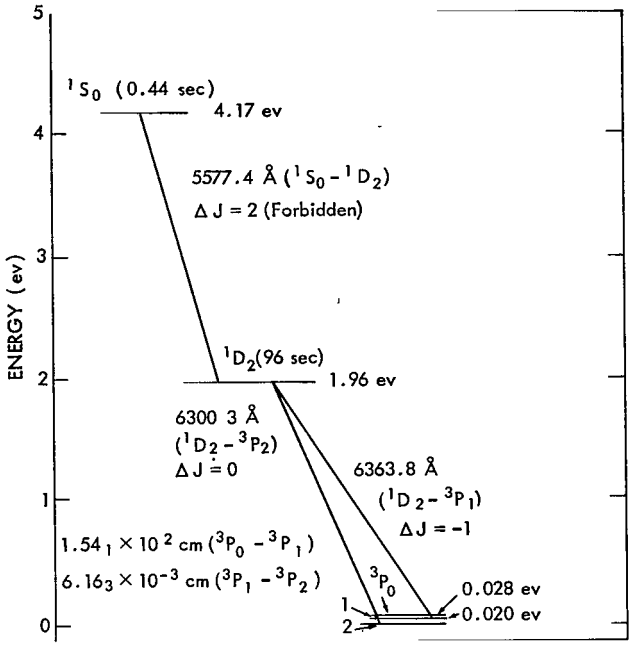

Figure 2—Energy levels of the neutral oxygen atom.

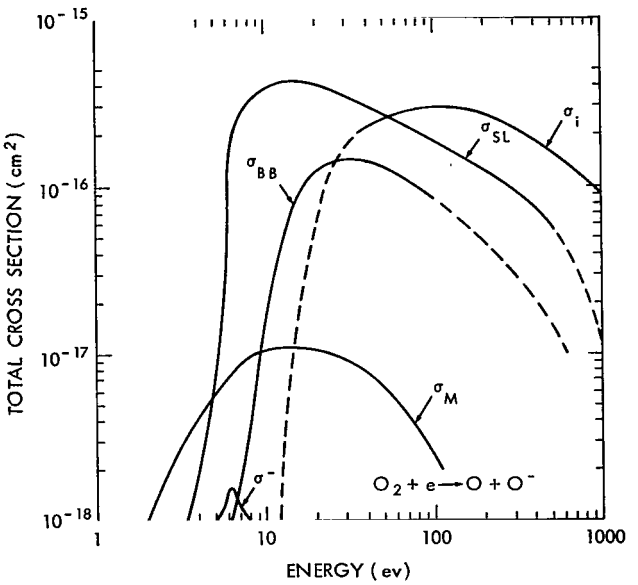

Figure 3—Total cross sections of O_2-dissociation by electron impacts. Reactions 1, 2, and 3 are indicated by σ^-, σ_{SL}, and σ_i, respectively. The previous calculation for Reaction 2 (Maeda, 1962, 1963a) is indicated by σ_M, whereas the calculation for Reaction 2 (Bauer and Bartky, 1965) by the classical theory is indicated by σ_{BB}.

The peak occurring around 6.5 ev undoubtedly corresponds to Reaction 1.

The major peak occurs at 8.4 ev and is due to dissociation from the excited state ($B^3\Sigma_u^-$). Dissociation from this level will lead to one atom in the ^3P ground state and one metastable ^1D atom (Figures 1 and 2). The peak at 9.0 ev results from dissociation of the $^1\Delta_u$ state leading to two ^1D atoms. Other peaks up to the first ionization potential at 12.04 ev McGowan et al. (1964), are also discernible. Schulz estimated the cross section and found an approximate value of 1.9×10^{-18} cm^2 at the 8.4 ev peak. The cross section has also been estimated chemically (Gockler and Wilson, 1932; Massey and Burhop, 1956). From an analysis of dc discharges in oxygen gas, Thompson (1961) estimated that the cross section for the dissociation of oxygen by electrons of energy greater than 14 ev is at least an order of magnitude greater than that for excitation to the $^1\Delta_g$ state.

The most recent experimental work on the cross section for dissociation of oxygen by electrons of energy greater than 20.0 ev has been accomplished by Lassettre (1959), who found that the cross section for dissociation by electrons of 500 ev incident energy was 10 percent of the total cross section. Lassettre et al. (1964) have shown that the cross section for energy loss at 8.44 ev by a 500-ev electron is 4×10^{-16} cm^2. Most of the dissociations result from this reaction, which is a source of O (^1D).

The oscillator strength, derived from the experimental data at 500 ev together with the Born approximation was used by Silverman and Lassettre (1964) to derive the dissociation cross section

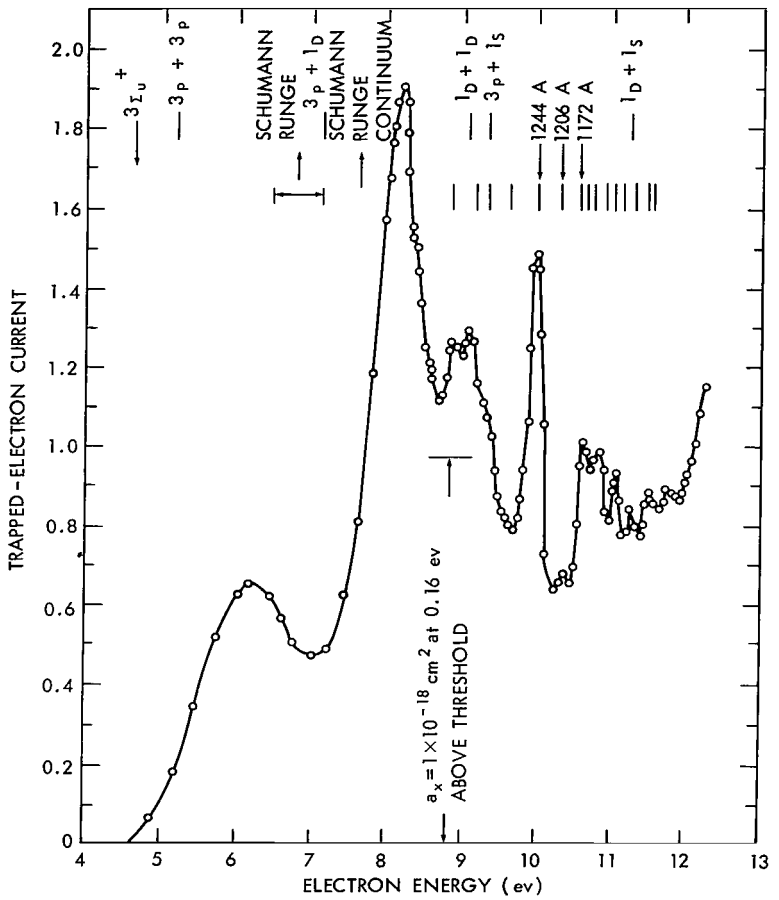

Figure 4—The excitation spectrum of molecular oxygen by electron impact between 4 and 12 ev compared with optical absorption bands.

as a function of incident electron energy. This cross section as a function of energy is reproduced in Figure 3. Also shown is the result of a calculation by Bauer and Bartky (1965) based on the classical theory of Gryzinski (1959) and employing the potential energy diagram (Figure 1) given by Gilmore (1964). Silverman and Lassettre (1964) regard their calculations as a lower bound on the dissociation cross section since only one transition is included. It should be noted that O_2-dissociation by electron impact is far larger than that of photodissociation in the same energy range. Figure 3 also gives the cross sections employed by Maeda (1962, 1963).

No information is available on the dissociation of ozone by electron impact. It will be assumed for the purposes of calculation that the cross section is as large as that given for O_2.

Reaction 3 is the dissociative ionization of oxygen. Frost and McDowell (1958) studied reactions of this type and found that as the colliding electron energy increases, not only O^+, but also O^-, O, and O^{++} are produced.

The cross section, σ_i, for O_2 ionization as measured by laboratory experiments is also shown in Figure 3 (Tate and Smith, 1932). The dashed curve at the low energy end of these data is an extrapolation assuming that the ionization cross section vanishes below the O_2 ionization potential.

AURORAL DISSOCIATION OF ATMOSPHERIC OXYGEN MOLECULES

Dissociation by Monoenergetic Electrons

The energy of most auroral electrons is between 5 and 50 kev, except for occasional hard-spectrum auroral electron events (McIlwain, 1960; Chamberlain, 1961, p. 269; Hultquist, 1964; Mann et al., 1963). Since the results of calculations made for monoenergetic electrons can be

applied to more general cases of different energy spectra, computations are performed first for several cases of monoenergetic electrons.

Any charged particle entering the earth's atmosphere follows a spiral orbit along a geomagnetic line of force. It can be shown, however, that if the magnetic field is uniform and vertical, the effect of spiral motion on the diffusion of charged particles in the atmosphere can be disregarded except for the estimation of the horizontal spread in the atmosphere (Maeda and Singer, 1961; Maeda, 1962; 1963). These charged particles, entering a denser atmosphere, simultaneously undergo multiple Coulomb scattering and energy-loss by collisions with air molecules in the upper atmosphere.

Because of the small mass of electrons, angular spreads of scattered electrons at each collision are very large compared with those of protons or heavier particles of the same velocity. Energy loss of electrons at each collision fluctuates wildly, causing the so-called straggling effect in their residual range, i.e., the penetration depth. Because of the statistical nature of these scatterings and energy losses, diffusion of electrons into the atmosphere has not been calculated rigorously until recently (Spencer, 1959; Rees, 1963; Maeda, 1965 a,b).

The rate of dissociation of atmospheric oxygen, $J_d(z, E_0)$, by monoenergetic incident electrons, E_0, at the altitude z, can be given by

$$J_{de}(z, E_0)dz = \int_0^{E_0} N(z) \left[\int_{E_c}^{E_0} \sigma_d(W)\, j_e(W, E, z)\, dW \right] i(E, E_0\, z)\, dE \cdot dz \quad , \tag{4}$$

where

$N(z)$ is the number density of molecular oxygen at the altitude z, (cm^{-3});

$\sigma_d(W)$ is the differential cross section of O_2-dissociation by electrons with energy W (cm^2, W in kev) and shown in Figure 3 by σ_{SL}, σ_M, and σ_{BB};

$j_e(W, E, z)$ is the number of secondary electrons of energy between W and $W + dW$, produced by electrons of energy E per unit thickness of air at the altitude z (cm^{-1}, z in km);

$i(E, E_0, z)$ is the number of electrons with energies between E and $E + dE$ at the height z, corresponding to the incident energy E_0, i.e., the differential energy spectrum of electrons in energy E and $E + dE$ at the altitude z, in the atmosphere normalized to the incident total flux of monoenergetic electrons of E_0 (cm^{-2} sec^{-1});

and

E_c (5 ev) is the threshold energy for O_2-dissociation.

The terms inside the square bracket of the integrand (Equation 4) can be written as:

$$\int_{E_c}^{E} \sigma_d(w)\, j_e(W, E, z)\, dW \simeq \sigma_t \cdot j_t(E) \cdot \rho(z) \quad , \tag{5}$$

where

$$\sigma_t = \frac{1}{W_e} \int_{E_c}^{\infty} \sigma_d (W)\, dW \ , \tag{6}$$

W_e ($\simeq 20$ ev) is the effective energy for O_2-dissociation,

$\rho(z)$ is the density of air (g/cm^3) at the altitude z (km),

and

$j_t(E)$ is the number of secondary electrons per primary electron with energy E (kev) per unit thickness of air (g/cm^2).

This is shown in Figure 5 as a function of E (kev). The curve below 1 kev is derived from the experimental data for O_2 and N_2 (Tate and Smith, 1932); and the residual portion, particularly above 10 kev, is computed by the following formula:

$$j_t(E) = \frac{k(E)}{V_0} \ , \tag{7}$$

where $V_0 \approx 32$ ev (Rossi, 1952, p. 47), and $k(E)$ is the rate of ionization loss of electrons with energy E in air given by the Bethe formula (Wu, 1960, p. 17).

The differential spectrum of electrons, $i(E, E_0, z)$, at the altitude z in Equation 4 is computed from $i(E, E_0, x)$, the spectrum at the atmospheric depth x, by making use of x-z relation for the CIRA-atmosphere (1965). If the ionization loss, Coulomb scattering and the effect of straggling are to be taken into consideration simultaneously, then $i(E, E_0, x)$ can be calculated only by the Monte Carlo method. In the present calculations, $i(E, E_0, x)$ is expressed by an analytic formula (Appendix B). A comparison of this expression with the result obtained by the Monte Carlo calculation is shown in Figure 6 for the case of vertically incident monoenergetic electrons; $E_0 = 20$ kev. The total intensity $I(E_0, \xi)$ is also expressed by an empirical formula, (Appendix B), which is shown in Figure 7 with results obtained by the Monte Carlo calculation (for $E_0 = 20$ kev). In Figure 7, the Monte Carlo result of the total energy flux variation with penetration depth in air $E(\xi)/E_0$ is also plotted against $\xi = x/r_0$.

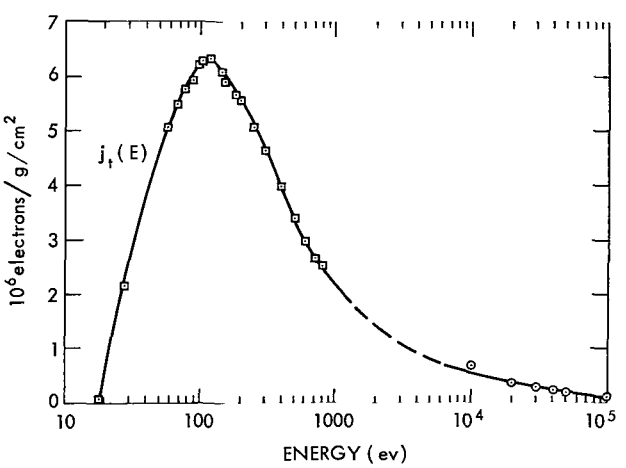

Figure 5—The number of secondary electrons per unit thickness of gas (O_2 and N_2, in g/cm) per electron of energy E (kev).

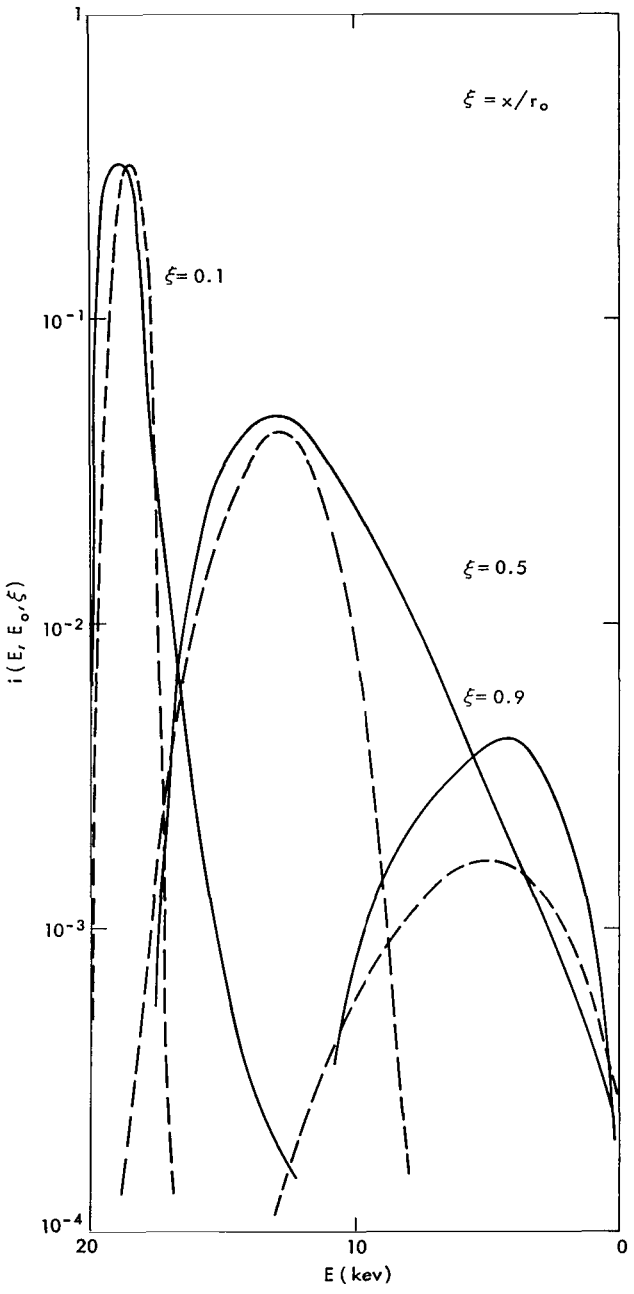

Figure 6—Comparison of $i(E, E_0, x)$ given by Equation B6 (dashed lines) and that of Monte Carlo calculation for the vertically incident monoenergetic electrons of E_0 = 20 kev (full lines).

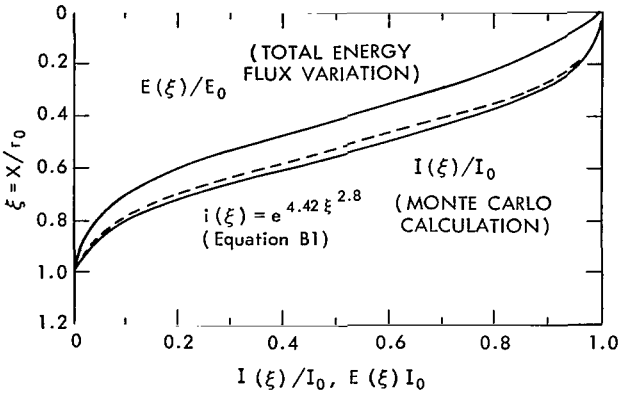

Figure 7—Variations of the total intensity of vertically incident monoenergetic electrons with atmosphere depth,

$$I(E_0\,\xi) = \int_0^{E_0} i\,(E,\ E_0\,\xi)\,dE$$

where $\xi = X/r_0$, ($r_0 = 9.824 \cdot 10^{-4}$ g/cm^2 for E_0 = 20 kev).

Final results of $J_{de}(z)$ cm^{-3} sec^{-1} are shown in Figure 8, as a function of altitude z (km) for vertically incident monoenergetic electrons with an initial energy range of 5 kev $\leq E_0 \leq$ 1 Mev.

By using the approximation (Equation 5), the right-hand side of Equation 4 is written as:

$$J_{de}(z, E_0)\,dz = \sigma_t \cdot N(z)\,\rho(z) \int_{E_0}^{E} j_t\,(E) \cdot i(E, E_0, z)\,dE\,dz \quad . \quad (8)$$

As can be seen from this expression, $J_{de}(z)$ is proportional to σ_t, the total cross section of O_2-dissociation by electron impact. The scale of the abscissa $J_{de}(z)$ in Figure 8 should be read, therefore, by multiplying a factor α, for different cases of reactions which are indicated by Equations 1, 2, and 3. The factor, α, and the effective energy W_e (ev) for these reactions and cross sections are shown in Table 1. From this table one can see that the application of the Lassettre cross section increases the dissociation rate

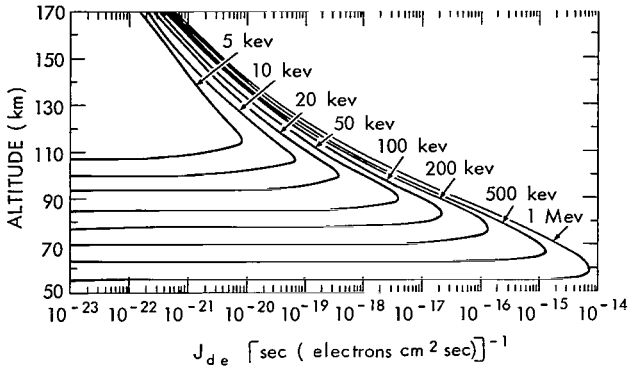

Figure 8—Rate of O_2-dissociation by monoenergetic auroral electrons (with energy E_0) as a function of altitude z (km) for 5 kev $\leq E_0 \leq$ 1 Mev.

Table 1

Multiplication Factors, Cross Sections, and Effective Energies for Reactions 1, 2, and 3.

Reactions	Cross Section (Figure 3)	α†	$\overline{W}_e$ (ev)‡
1	σ_M	0.1	10
	σ_{SL}	1.0	80
	σ_{BB}	0.5	80
2	σ_i	2.0	150
3	σ^-	$<10^{-3}$	6

†Multiplication factors for $J_{de}(z)$ as shown in Figure 6.
‡Effective energies for reactions and cross sections.

by a factor of 10 above that employed by Maeda (1963). The Lassettre cross section value will be applied in all subsequent calculations of the dissociation effects of auroral electrons.

Dissociation by Auroral Electrons with Exponential Spectra

It has been reported that the energy distribution of the primary auroral electrons, $i(E_0)$, is consistent with the following form of exponential spectrum rather than the single power-of-energy formula; a monoenergetic distribution, $\delta(E - E_0)$, is a fairly good approximation in most cases (McIlwain, 1960; Brown, 1964):

$$i(E_0) = i_0 \exp\left(-\frac{E_0}{E_a}\right), \tag{9}$$

where E_a is a constant (kev).

The effect of the energy spectrum of the rate of dissociation can be calculated by making use of previous results for monoenergetic electrons as follows:

$$J_D(z) = \frac{\int_0^\infty J_{de}(z, E_0) \exp\left(-\frac{E_0}{E_a}\right) dE_0}{\int_0^\infty \exp\left(-\frac{E_0}{E_a}\right) dE_0} \simeq \frac{1}{E_a} \sum_{i=1}^{\infty} J_{de}(z, E_0^i) \exp\left(-\frac{E_0^i}{E_a}\right) \Delta E_0^i, \tag{10}$$

where $J_{de}(z, E_0^i)$ is given by Equation 8 and shown in Figure 8 as a function of the altitude z (km).

In Figure 8 E_0^i is taken as a parameter for the range from 5 kev to 1 Mev, and the altitude z is indicated in the abscissa. Computation of $J_D(z)$ is shown in Figure 9 for E_a = 5 and 100 kev.

PHOTOCHEMICAL REACTIONS FOR MESOSPHERIC OZONE AND ATOMIC OXYGEN

The amount of ozone above 50 km comprises less than 1 percent of the total ozone content in a vertical column of the atmosphere. However, a knowledge of its distribution and time variation is important in the study of the dynamics of the mesosphere, as well as airglow phenomena such as the OH-band emission in the lower mesosphere (Bates and Nicolet, 1950; Wallace, 1962; Hunt, 1966 b). The role of ozone in the ionosphere as a possible attaching agent to form O_3^- has been discussed in terms of the twilight behavior of PCA events (Reid, 1964). The altitude distribution and temporal variation of atomic oxygen are also important from both the ionospheric and aeronomical standpoints. In this section, the time-dependent equations governing the distribution of ozone and atomic oxygen will be solved for an oxygen atmosphere. Before investigating the effect of auroral particles, calculations will be performed for both an equatorial and polar atmosphere under the influence of solar radiation. Since the equatorial distribution has been discussed by many investigators, the present calculation scheme can be compared with the results of others.

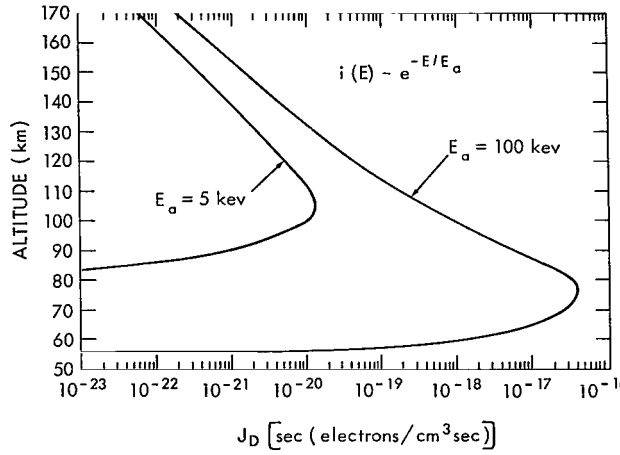

Figure 9—Rate of dissociation by auroral electrons with energy e^{-E_0/E_a} vs altitude z.

Equations and Constants

Principal reactions for ozone formation and destruction are shown in Table 2. The element M in the three-body collision is not necessarily oxygen; M is any atom or molecule which balances the energies and momentum in the colliding reaction. The number density [M] is, therefore, given by the total number density of air. Although the importance of reactions involving hydrogen has been treated by Wallace (1962) and shown to be necessary to explain quantitatively the ozone distribution more recently derived by Hunt (1966 b), only a pure oxygen atmosphere will be considered in the present investigation.

Corresponding to reactions shown in Table 2, time variations of odd-oxygen allotropes are given by the following two equations together with a similar equation for O_2:

$$\frac{d[O_3]}{dt} = k_{12}[O][O_2][M] - k_{13}[O][O_3] - J_3[O_3] \tag{11}$$

and

$$\frac{d[O]}{dt} = 2J_2[O_2] + J_3[O_3] - k_{12}[O][O_2][M] - k_{13}[O][O_3] - k_{11}2[O]^2[M] , \tag{12}$$

Table 2

Principal Reactions for Atmospheric Ozone Formation and Destruction.

Ozone formation

$$O + O_2 + M \xrightarrow{k_{12}} O_3 + M$$

Ozone destruction

$$O + O_3 \xrightarrow{k_{13}} 2O_2$$

Atomic oxygen recombination

$$O + O + M \xrightarrow{k_{11}} O_2 + M$$

Dissociation of molecular oxygen

$$O_2 + h\nu \xrightarrow{\sigma_2} O + O \text{ for } \lambda < 2424\text{Å}$$

$$O_2 + e \xrightarrow{\alpha_2} O + O + e \text{ for } E > 5 \text{ ev}$$

Ozone dissociation

$$O_3 + h\nu \xrightarrow{\sigma_3} O + O_2 \text{ for } \lambda < 11800\text{Å}$$

$$O_3 + e \xrightarrow{\alpha_3} O + O_2 + e \text{ for } E > 1 \text{ ev}$$

where $[O]$, $[O_2]$, and $[O_3]$ are the number densities of atomic oxygen, molecular oxygen, and ozone, respectively, and $[M]$ is the total number density. A summary of the values of the rate coefficients k_{11}, k_{12} and k_{13} employed in the present calculations is given in Table 3 together with the most recent laboratory determinations. The table shows that the reaction rate changes with atmospheric temperature, which is a function of altitude, latitude, and season. Since the main purpose of the present calculation is to determine the basic character of variation rather than to investigate many possible cases, the effect of atmospheric temperature will be ignored here and discussed separately.

The total rates of O_2-dissociation by solar UV-radiations and auroral electrons are given

Table 3

Rate Coefficients.

Reaction	Present calculation	Rate	
k_{11} cm^6 sec^{-1}	3×10^{-33}	3×10^{-33}	(Reeves et al., 1960)
k_{12} cm^6 sec^{-1}	5×10^{-34}	8×10^{-35} exp (445/T)	(Benson & Axworthy, 1965)
k_{13} cm^3 sec^{-1}	2.3×10^{-15}	5.6×10^{-11} exp (-285°/T)	(Benson & Axworthy, 1965)

by J_2 and J_3 for O_2 and O_3. The expression for the particle dissociation rate is given by Equation 8. The photodissociation rate is

$$J_{pi}(z) = \sum_{\lambda} \sigma_{i\lambda} Q_{\infty\lambda} \exp(-\tau_\lambda) \ (\text{sec}^{-1}) \ , \qquad (13)$$

where $\sigma_{i\lambda}$ is the dissociation cross section as a function of wavelength for a particular constitutent oxygen ($i = 2$) and ozone ($i = 3$). The intensity of solar radiation (Q_∞) outside the earth's atmosphere is represented in units of photons cm^{-2} sec^{-1} unit wavelength^{-1}. The optical depth τ_λ represents the product of the absorption cross section and total number of absorbing molecules between height z and the sun and is a function of time.

The resulting differential equations are solved with a computer. Since some of the reactions are too fast to permit stable integration by the Runge-Kutta method, a more stable, linearized

finite difference scheme is utilized in the present computation (Appendix C).

Vertical Distributions of Atmospheric Ozone and Atomic Oxygen

Equatorial Region

In Figure 10, the diurnal variation of atomic oxygen, [O] in cm^{-3}, in the equatorial atmosphere at summer solstice is shown for each altitude from 50 to 100 km at 10-km intervals. The variation of the vertical distribution of atomic oxygen as a function of altitude with time as a parameter is given in Figure 11, where increasing phase and decreasing phase of the

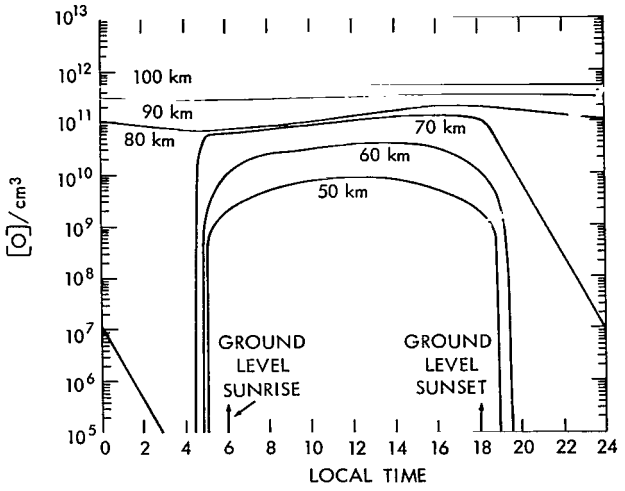

Figure 10—Diurnal variation of atomic oxygen/cm^3 at each level from 50 km with 100 km at 10-km intervals in equatorial atmosphere at the summer solstice.

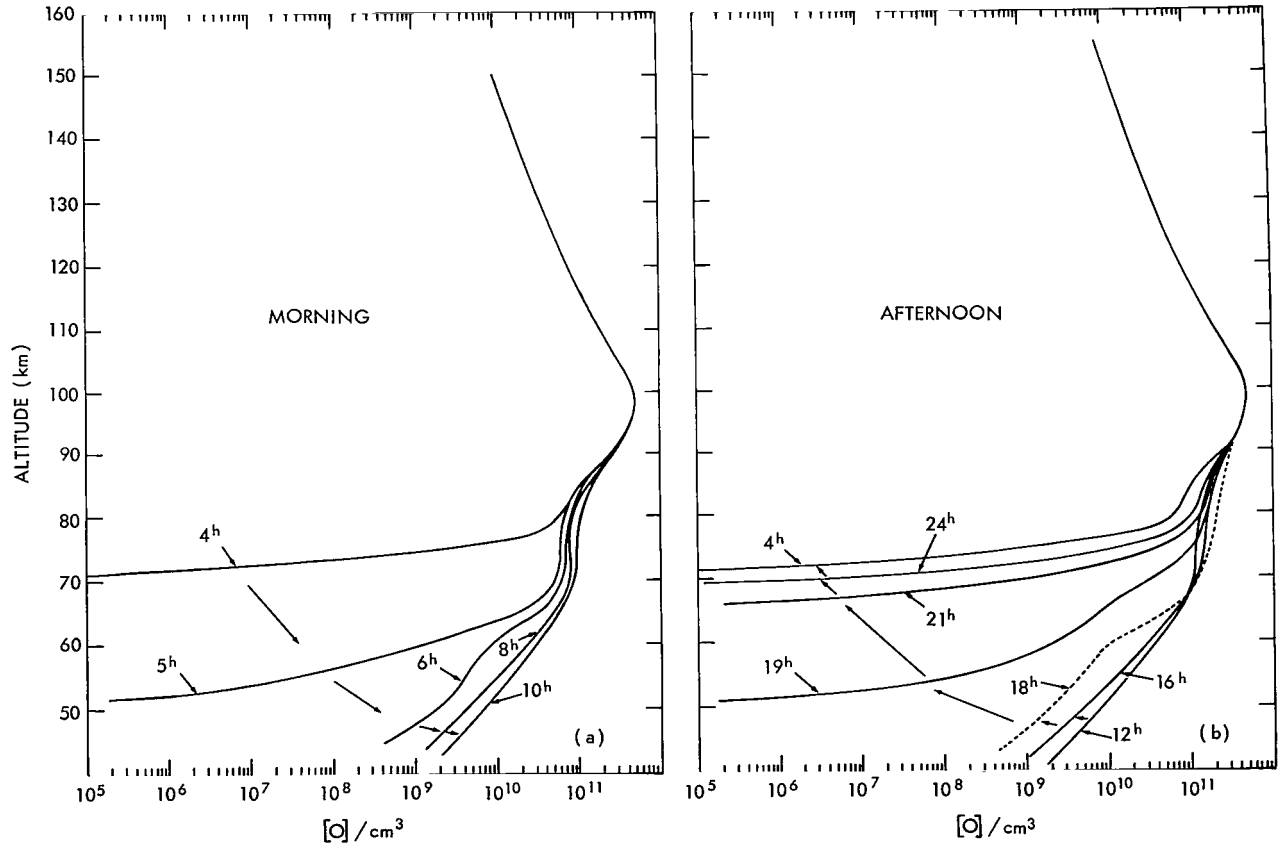

(a) Increasing phase after sunrise.

(b) Decreasing phase in the afternoon.

Figure 11—Diurnal variation of vertical distribution of atomic oxygen.

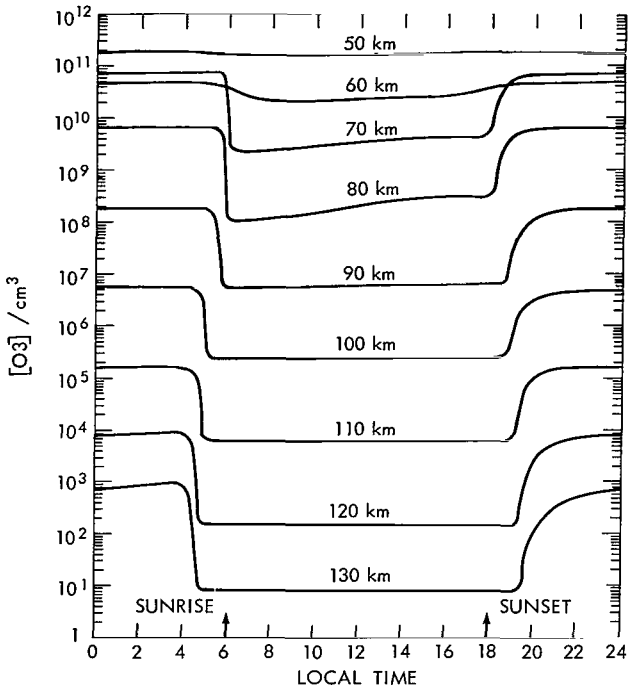

Figure 12—Diurnal variation of ozone at each level corresponding to the oxygen-atom variations shown in Figure 10, in the equatorial atmosphere at summer solstice.

diurnal variation are presented separately, i.e., (a) for morning (increasing phase), (b) for afternoon (decreasing phase). Figure 12 shows the variations of ozone at each altitude corresponding to the oxygen atom variations shown in Figure 10. The variation of vertical ozone distribution with time as a parameter is given in Figure 13, where the increasing phase, which starts after the sunset, and the decreasing phase after the sunrise are shown separately in (a) and (b), respectively.

Comparisons of observations and other calculations are shown in Figure 14. There is reasonable agreement between daytime observations and Hunt's calculation for daytime distribution with respect to the oxygen-hydrogen atmosphere between 50 and 80 km. Although Hunt's conclusion, that a pure oxygen atmosphere leads to an excess of ozone, can be confirmed by the present calculation for the altitude below 80 km, his equilibrium (daytime) ozone distribution above the 80-km level is too large. It should be noted that the oxygen atom concentration above 90 km used by Hunt (1966) is nearly one order of magnitude higher than the recent direct measurements (Golomb et al. 1965).

On the other hand, nighttime enhancement of mesospheric ozone, with a maximum of about 70 km, obtained by present calculation and by Hunt's pure oxygen atmosphere results shows better

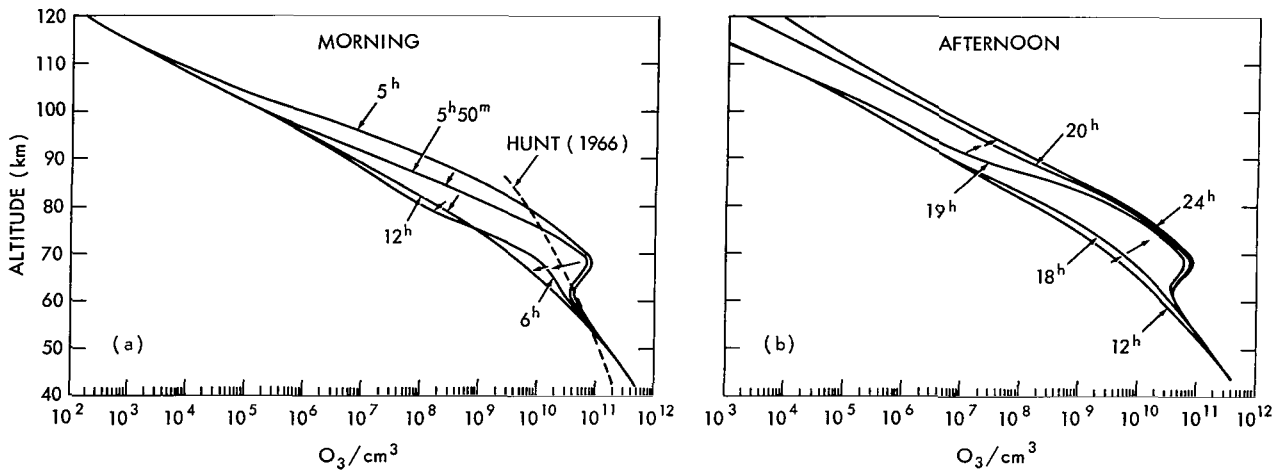

(a) Increasing phase.

(b) Decreasing phase.

Figure 13—Vertical cross section of temporal variation of ozone shown in Figure 12.

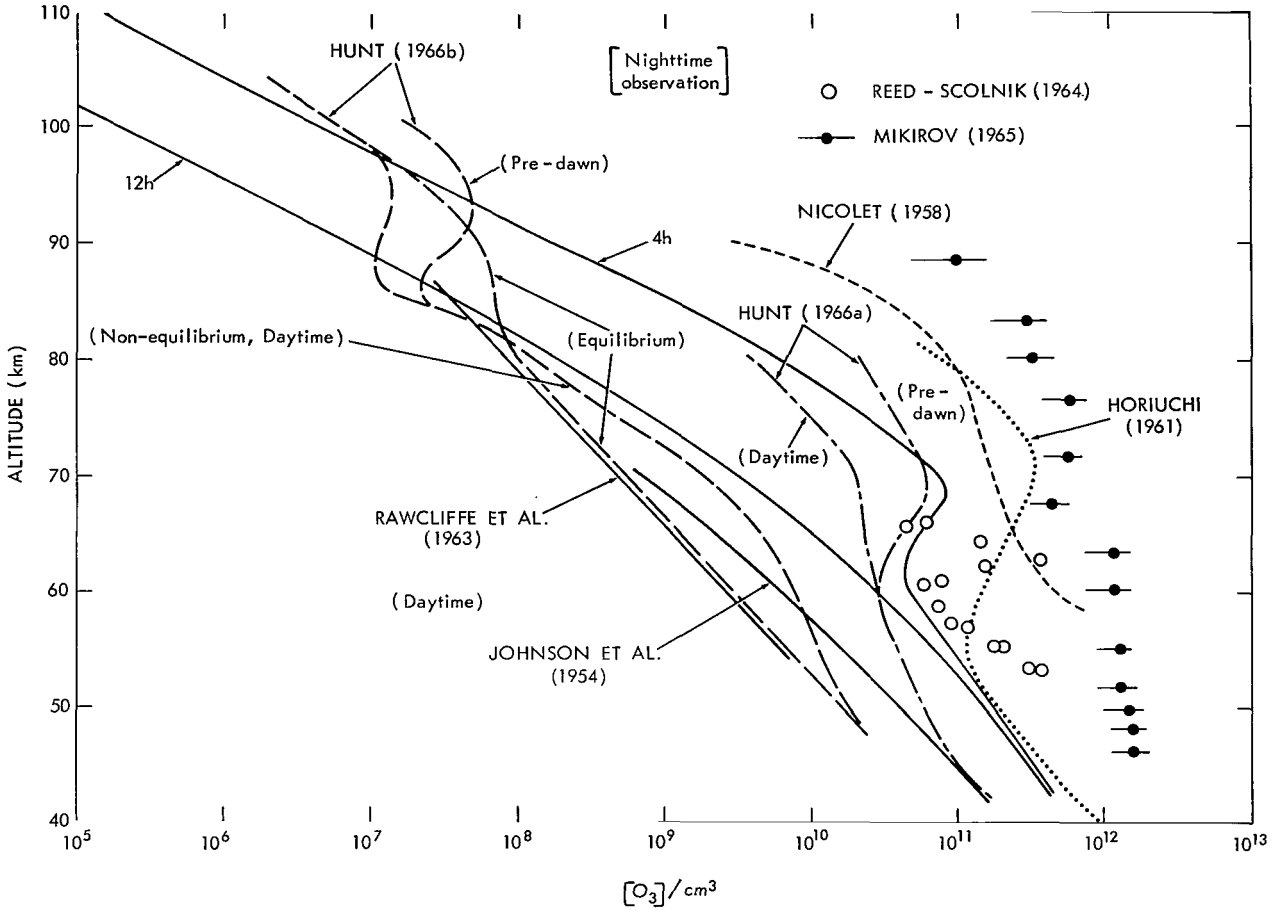

Figure 14—Comparison of observed values and theoretical results of ionospheric ozone distributions at the daytime equilibrium and nighttime enhancement.

agreement with observations that oxygen-hydrogen atmosphere results. Since the data of Reed and Scolnik require some corrections for the spectrum-line widths with altitude,* detailed comparison with data seems premature. It should be noted, however, that Mikirov's observation indicates far larger nighttime enhancement than present estimation and rather agrees with Nicolet's and Horiuchi's estimations. Further nighttime mesospheric ozone measurements are necessary to discuss these differences. It has been noted that below 80 km, the nighttime ozone concentrations are unaffected by hydrogen reactions, since in the absence of sunlight the free hydrogen concentration falls to insignificant values. Therefore, unless there is significant dissociation of water vapor by electron impact, a pure oxygen atmosphere should be sufficiently good approximation for use in describing auroral events occurring at night.

*Edith Reed, Private communication, 1966.

From Figures 10, 11, 12, and 13, the relaxation time of the atmospheric oxygen atom, τ_1 (sec), and that of ozone τ_3 (sec) can be obtained for the temperature-independent rate coefficients of Table 3. The time constants are compared in Figure 15, with Hunt's results (1964).

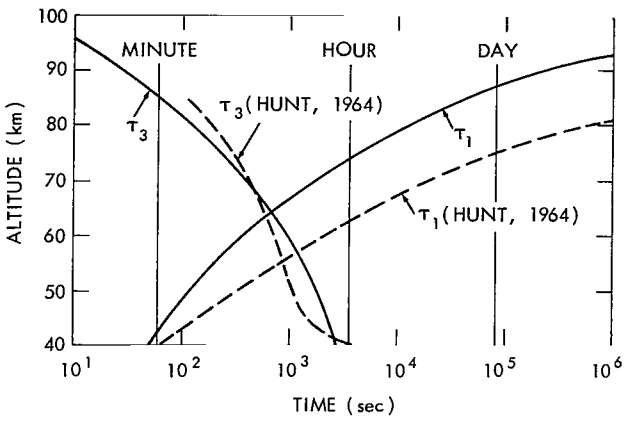

Figure 15—Time constants of atmospheric oxygen-atom τ_1 (sec) and of ozone, τ_3 (sec), and comparison with Hunt's (1964) results.

Polar Region

The distribution of constituents in the polar winter mesosphere is particularly difficult to describe because of prolonged twilight conditions. In Figure 16(a) and (b), corresponding to the solar declination, δ = 0 degrees (equinox) and δ = -10 degrees, respectively. On this basis, one would expect very low atomic oxygen concentration in the winter polar mesosphere, if there is no subsidence and horizontal transport from the sun-lit latitudes. Kellogg and Schilling (1951) considered adiabatic heating to be due to air-subsidence at least at the rate of 1 km per day in an effort to explain the increase in temperature of the winter mesosphere, which is warmer than that in summer. Later Kellogg (1961) suggested that atomic oxygen created at heights above 80 km would be carried polewards to the dark hemisphere, where subsidence of the oxygen would increase the heating rate by the exothermic (5.08 ev) three-body recombination reaction. Young and Epstein (1962) have shown that rates of subsidence of 0.2 cm per sec are sufficient to account for the observed heating provided that the atomic oxygen concentration at 115 km is 1.5×10^{11} cm^{-3} or greater. On the basis of this density, it was shown that atomic oxygen densities of the order of 10^{12} cm^{-3} can be obtained at 70 km. The value of the rate coefficient which was chosen for k_{13} in the calculation is, however, one order of magnitude larger than that utilized by Hunt (1966). It is also possible for diffusion to be active in redistributing the atomic oxygen concentration and ozone formed in the upper mesosphere and in the lower thermosphere; the effect of diffusion is estimated in Appendix A.

MESOSPHERIC OXYGEN DISTRIBUTION DURING AURORAL EVENTS

In Figure 9, the dissociation rates per incident electron have been given for two exponential spectra for e-folding energies, E_a = 5 and 100 kev. These spectra represent the limits for soft and hard spectrum of observable auroral electrons and can be used to establish the particle flux necessary to modify the atomic oxygen distribution in each instance. Such an estimate can be made by employing the time-independent solution of Equation 12 and solving for the flux necessary to overcome the decay terms. As can be seen from Figure 9, a spectrum with E_a = 5 kev can have no effect at altitudes of 80 km and below. However, if a flux is more than 5×10^5 electrons per cm^2 sec, the production rate can overcome recombination effects

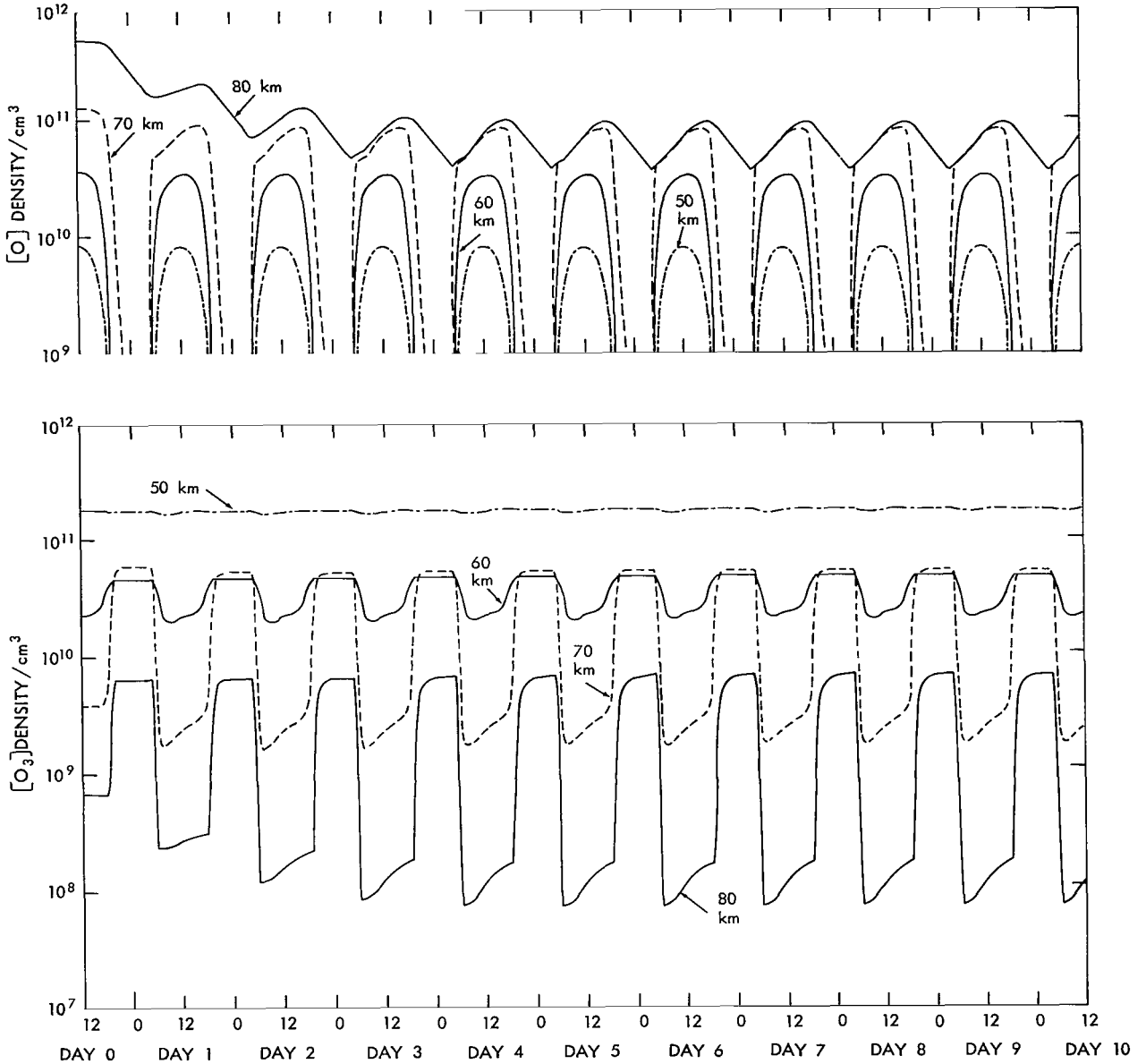

Figure 16(a)—Temporal variation of ozone and atomic oxygen in the polar hemisphere at the geographic latitude λ = 70 degrees and solar declination δ = 0 degrees (equinox).

at 70 km for the E_a = 100 kev case. It is, therefore, the hard spectrum events that are of importance in modifying the atmosphere below 80 km, where atomic oxygen has a short lifetime (Figure 15). Most bright auroras, however, are not of this hard spectrum type, but are characterized by the soft spectrum with E_a's of 5 to 10 kev and by the fluxes of 10^9 to 10^{12} electrons per cm^2 sec (McIlwain, 1960; Brown, 1966). Such events are not important unless the duration is of the order of several hours, which might affect the atomic oxygen distribution above 80-km level, since the lifetime of atomic oxygen is long above these altitudes. Hard spectrum events of the type sufficient

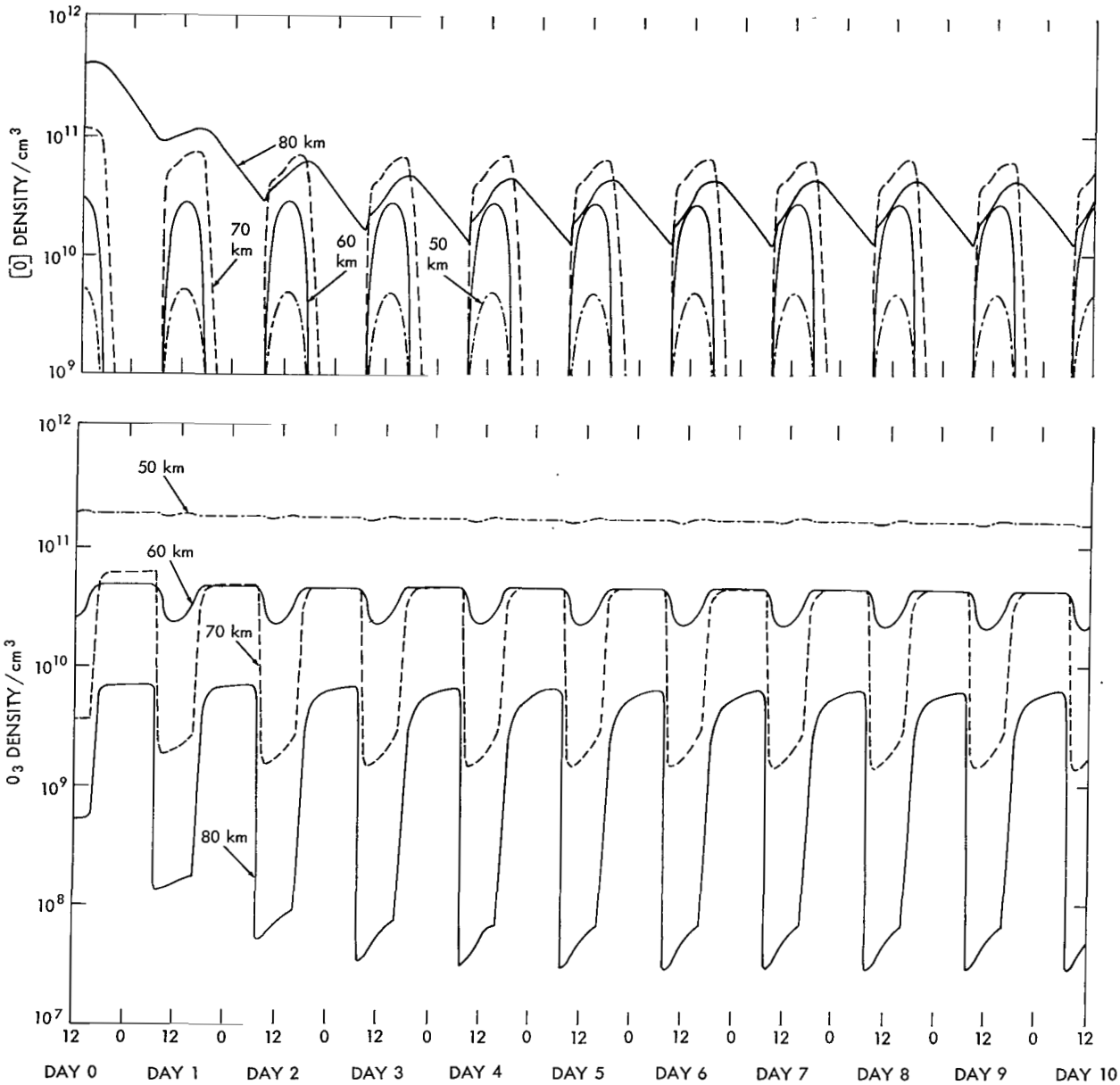

Figure 16(b)—Temporal variation of ozone and atomic oxygen in the polar hemisphere at the geographic latitude λ = 70 degrees and solar declination δ = -10 degrees.

to affect the atomic oxygen concentration have been reported by Bailey, et al. (1966) on the basis of forward-scatter radio-propagation data and balloon measurements of auroral Bremsstrahlung (Brown, 1966). Such events, referred to as relativistic electron precipitation events, or REP's appear to be characterized by E_a's between 60 and 150 kev and fluxes between 10^6 and 2×10^4 electrons per cm^2 sec. There is also satellite evidence of hard spectra auroral electrons (Mann, et al., 1963).

In the present calculation, Equations 11, 12, and 13 are solved by the method described previously (and shown in Appendix C) for a latitude of 70 degrees during equinox. In addition to the small

solar photodissociation rate, particle fluxes are superimposed. As stated previously the cross section of O_3 dissociation by electron impact is not known. However, the dissociation cross section of ozone (a triatomic molecule) by electron impact should be larger than that of the diatomic molecule. Therefore, two values have been assigned to the ozone dissociation rate; i.e., $J_3 = 10^2 J_2$ and $J_3 = J_2$. It will be shown that the effect of auroral events on the temporal and spatial variations of atmospheric ozone and oxygen are not drastically affected by the assumption of the O_3-dissociation rate unless it is assumed to be unreasonably small.

The following eight cases have been considered in the calculations: flux (intensity) of impinging auroral electrons $i_0 = 10^{11}$ to $i_0 = 10^5$ (cm^{-2} sec^{-1}); energy spectrum of auroral electrons

$$j(E_0) = j_0 \exp\left(-\frac{E_0}{E_a}\right), \tag{14}$$

where E_a = 100 kev (hard spectrum) and E_a = 5 kev (soft spectrum); and the ratio of dissociation rate of O_2 and of O_3, $J_3 = J_2 \times 10^2$ and $J_3 = J_2$. Duration of auroral bombardment was assumed to be 10 minutes and initiated at midnight for all calculations.

It was found that the soft spectrum case had essentially no effect even for large fluxes of incident electrons. Hard spectrum events of even short duration (1 minute or so) can give rise to significant enhancements at low altitudes. For instance, for a flux of 10^5 electrons per cm^2 sec a density 10^5 cm^{-3} atomic oxygen can be maintained at night at 60 km and for the same flux the density at 70 km, can reach densities of 10^8 cm^{-3}. The resulting atomic oxygen and ozone distributions for the hard spectrum case (E_a = 100 kev) are shown in Figures 17 (a through c) and 18 (a through c) for $J_3 = J_2 \times 10^2$ and $J_3 = J_2$, respectively, for the extreme case of $i_0 = 10^{11}$ cm^{-2} sec^{-1}.

From these figures, it can be seen that the atomic oxygen concentration is altered significantly below 80 km. In fact, there is an increase of concentration of five orders of magnitude at 70 km, which decays with time constant τ_1 indicated in Figure 15. The increase in O_3 is most significant around the 60 to 70-km level and is almost independent of the assumed ozone dissociation rate unless this is chosen to be negligibly small. From the foregoing, it is evident that for a hard spectrum auroral electron (E_a = 100 kev) and large incident flux

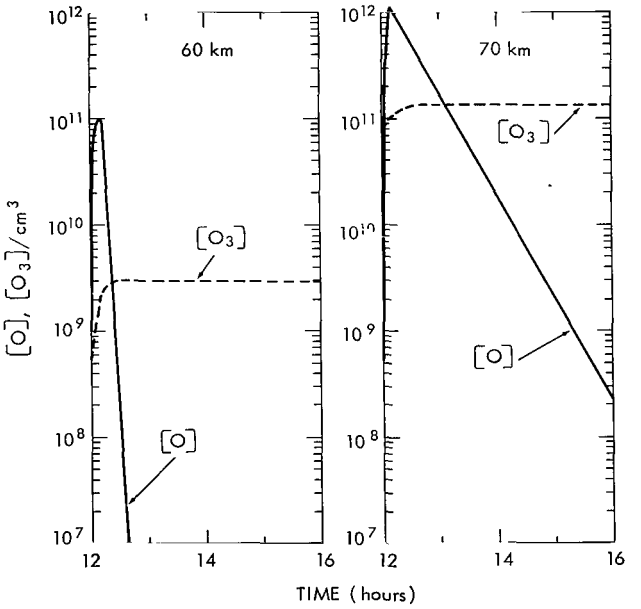

Figure 17(a)—Variation of the O and O_3 concentration during and after the hard spectrum electron precipitation at 60 and 70 km, for $J_3 = J_2 \times 10^2$ and $i_0 = 10^{11}$ cm^{-3} sec^{-1}.

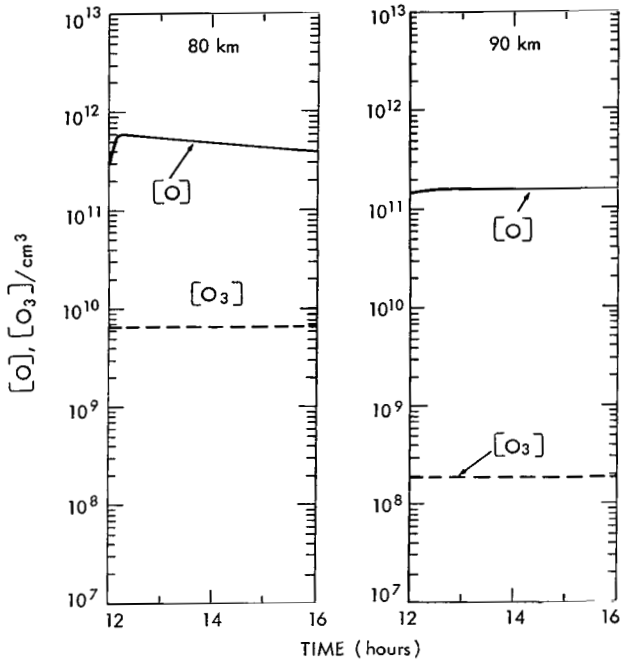

Figure 17(b)—Variation of the O and O_3 concentration during and after the hard spectrum electron precipitation at 80 and 90 km for $J_3 = J_2 \times 10^2$ and $I_0 = 10^{11}$ cm^{-3} sec^{-1}.

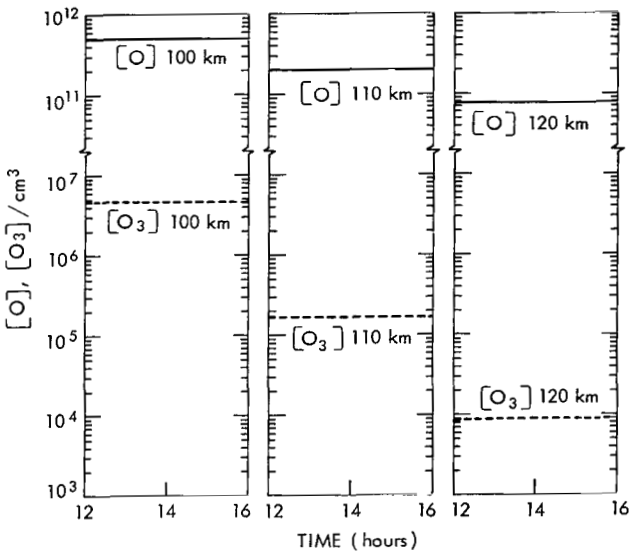

Figure 17(c)—Variation of the O and O_3 concentration during and after the hard spectrum electron precipitation at 100, 110, and 120 km for $J_3 = J_2 \times 10^2$ and $i_0 = 10^{11}$ cm^{-3} sec^{-1}.

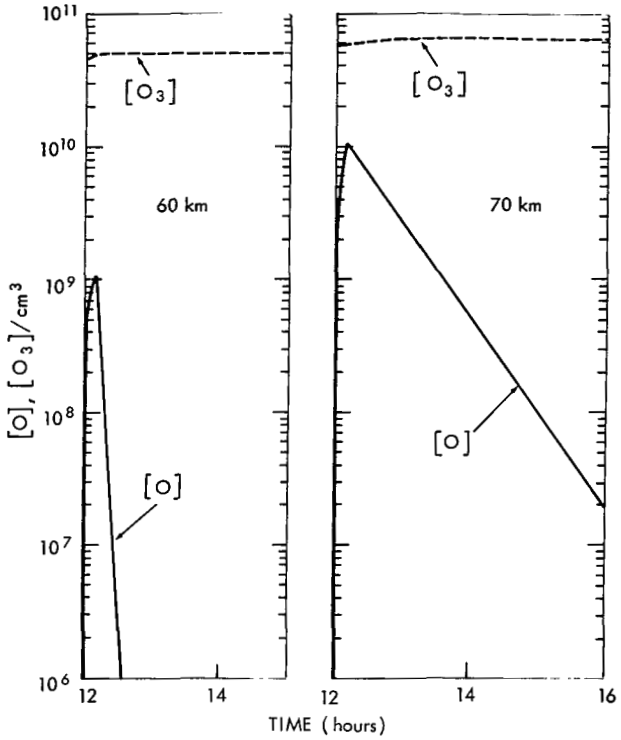

Figure 18(a)—Variation of the O and O_3 concentration during and after the hard spectrum electron precipitation at 60 and 70 km for $J_3 = J_2$.

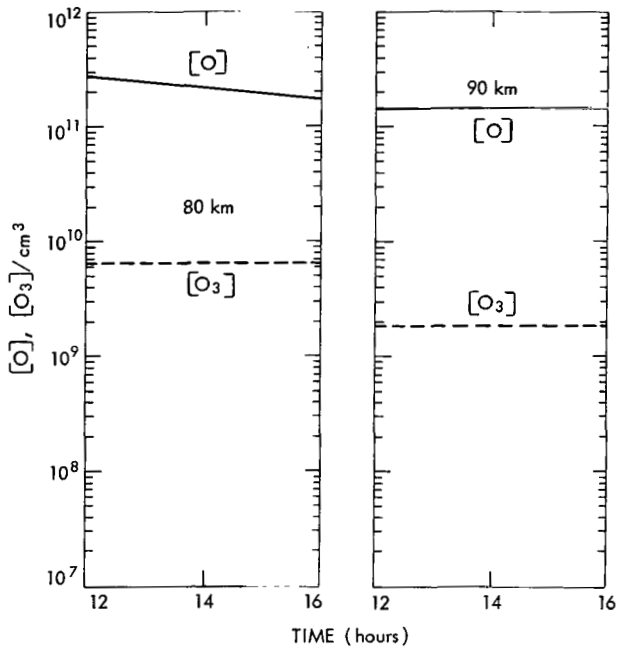

Figure 18(b)—Variation of the O and O_3 concentration during and after the hard spectrum electron precipitation at 80 and 90 km for $J_3 = J_2$.

($i_0 = 10^{11}$ cm^{-2} sec^{-1}), the profiles of atomic oxygen and, to a lesser extent, of ozone are substantially modified during and after the period of electron precipitation. Since the diffusion time of dissociated oxygen is long at these altitudes, the enhancement is confined within the horizontally narrow domain of particle precipitation (within bright auroras).

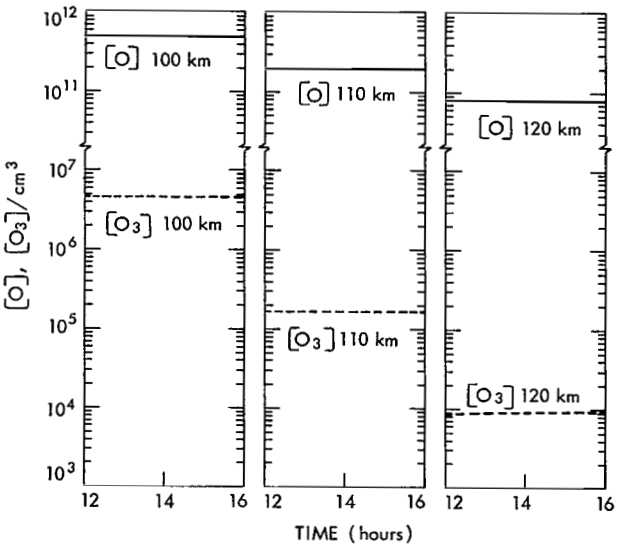

Figure 18(c)—Variation of the O and O_3 concentration during and after the hard spectrum electron precipitation at 100, 110, and 120 km for $J_3 = J_2$.

From the present calculation, it is seen that the effect of O_2 dissociation is significant only below the 80-km level for both processes of dissociations, i.e. by auroral particles as well as by solar UV-radiation. Since no auroral electrons with energy less than 100 kev penetrate below the 80-km level (Figure 8), the rate of auroral dissociation depends strongly on the amount of high energy electrons or on the spectrum of auroral electrons. In other words, if the spectrum is soft as seen in most bright auroras (McIlwain 1960, Brown 1966), no effects of auroral dissociation are detected. On the other hand, if the spectrum is hard, an increase of atomic oxygen below the 80-km level, together with a subsequent increase of mesospheric ozone, can occur. It should be noted, however, that hard spectra of auroral electrons appear generally in weak displays (Brown 1966). Durations should be, therefore, more than hours before the effects of auroral dissociation of atmospheric oxygens can be observable.

If local variations of auroral activities are considered, the intensity of the auroral electron, and its spectra change drastically within milliseconds and several hundreds meters of horizontal scale (O'Brien, 1964; Brown, 1966; Mozer and Bruston, 1966). The time constants of oxygen allotrope variations above stratosphere are, however, at least in the order of minutes (Figure 15). The intensities and spectra of auroral electrons to be compared to the present calculation are, therefore, those averaged over several minutes and many hundreds of kilometers in horizontal scale. In this respect, auroral effects on atmospheric oxygen are quite similar to those deduced from the auroral absorption measurements by riometer as far as time and horizontal scales are concerned.

Finally, the following can be regarded as one of the important differences between the effects of solar UV-radiations and those of auroral particles on the atmospheric oxygen; i.e., in the case of solar UV-dissociation, the increase of atomic oxygen is always accompanied by the decrease of ozone, while both oxygen atoms and ozone increase in the case of auroral dissociation. This is essentially due to the steep spectrum of solar UV-radiation in which the intensity of the Schumann-Runge region is nearly three orders of magnitude less than those ozone-destroying Hartley regions.

According to Akasofu (1964), the input energy flux of auroral particle is of the order of 80 ergs per cm^2 sec (the total energy deposit-rate, 8×10^{16} ergs per sec, divided by the total cross-sectional area exposed to incoming auroral electrons, 10^{15} cm^2). This figure is comparable to the energy flux of solar UV-radiation with wavelength shorter than 2000 Å (Hinteregger, 1965). It should be noted, however that the energy flux of bright aurora exceeds this figure more than several orders of magnitude, fluctuating within the order of milliseconds.

IONOSPHERIC EFFECTS OF OZONE AND ATOMIC OXYGEN ENHANCEMENT

When an auroral electron interacts with the atmosphere, it loses most of its energy through excitation and ionization. The resulting ionization leads to increased radio wave absorption during auroral electron precipitation, and in the case of proton flares, polar cap absorption events. An adequate description of these events depends on a knowledge of the electron distribution, which is dependent on the negative ion distribution in the D region. The species of negative ion is unknown at present. However, it is usual to assume O_2^- although O_3^- and NO_2^- have been suggested. The negative ion is formed initially by electron attachment. The species of negative ion may then be changed by charge transfer reactions, or the ion may be destroyed by a variety of processes. These include the very important associative detachment reaction

$$O_2^- + O \rightarrow O_3 + e \quad . \tag{15}$$

This reaction has figured in practically every theoretical treatment of the lower ionosphere both for the normal diurnal variation Aikin (1962) and for disturbed events such as PCA's (Whitten and Poppoff, 1962; Reid, 1966). Associative detachment was also utilized to explain auroral absorption events by Aikin and Maier (1963) who suggested that a modification of the atomic oxygen distribution by the incoming energies particle might change the negative ion density profile during such events.

Fehsenfeld et al. (1966) have recently measured the rate of Equation 15 and obtained a value of 3×10^{-10} cm^{-3} sec^{-1} which is more than sufficient to make this process dominant above photodetachment during the day. If only O_2^- is considered, the negative ion distribution will be controlled entirely by the atomic oxygen concentration. However, the possibility that O_2^- and O^- may charge-exchange with neutral species to form ions such as O_3^- and NO_2^- must be given consideration. Ferguson* has measured the rate of the reaction

$$O_3^- + CO_2 \rightarrow CO_3^- + O_2 \quad ,$$

and found it to have a rate of 3×10^{-10} cm^{-3} sec^{-1} so that ions of this species are a possibility as well as

$$O_3^- + NO \rightarrow NO_3^- + O \quad .$$

*E. E. Ferguson, Private communication, 1966.

It is evident that the distribution of O and O_3 can greatly influence the ionosphere wherever negative ions are of importance. The possibility exists that the negative ion distribution and perhaps the species is quite different between the normal D region, that affected by hard spectrum auroral electrons and PCA protons, simply because the distribution of ozone and atomic oxygen differs in the lower mesosphere during these circumstances.

CONCLUSIONS

The time-dependent photochemical equations describing the vertical distribution of ozone and atomic oxygen in a pure oxygen atmosphere have been solved for the equatorial and polar regions. The extended periods of twilight play an important role in the polar regions. Continuous sunlight can lead to an excess of atomic oxygen at altitudes where the atomic oxygen lifetime is greater than one day. For winter periods when the insolation is absent, appreciable atomic oxygen concentration cannot be maintained at altitudes below 80 km without a downward flow mechanism, such as subsidence or diffusion, or without a production mechanism, such as a large flux of energetic electrons.

It has been shown that the cross section for molecular oxygen dissociation by low energy electrons is quite large (Figure 3). Thus secondary electrons created during auroral particle precipitation into the atmosphere can modify the atomic oxygen and ozone distribution. If the energy spectrum of the auroral primary electrons is very hard such that the e-folding energy E_a is 50 kev or greater, mesospheric ozone and atomic oxygen concentrations around 60 to 70 km increase significantly (Figures 17 through 20). The majority of events are not of this type but are generally very

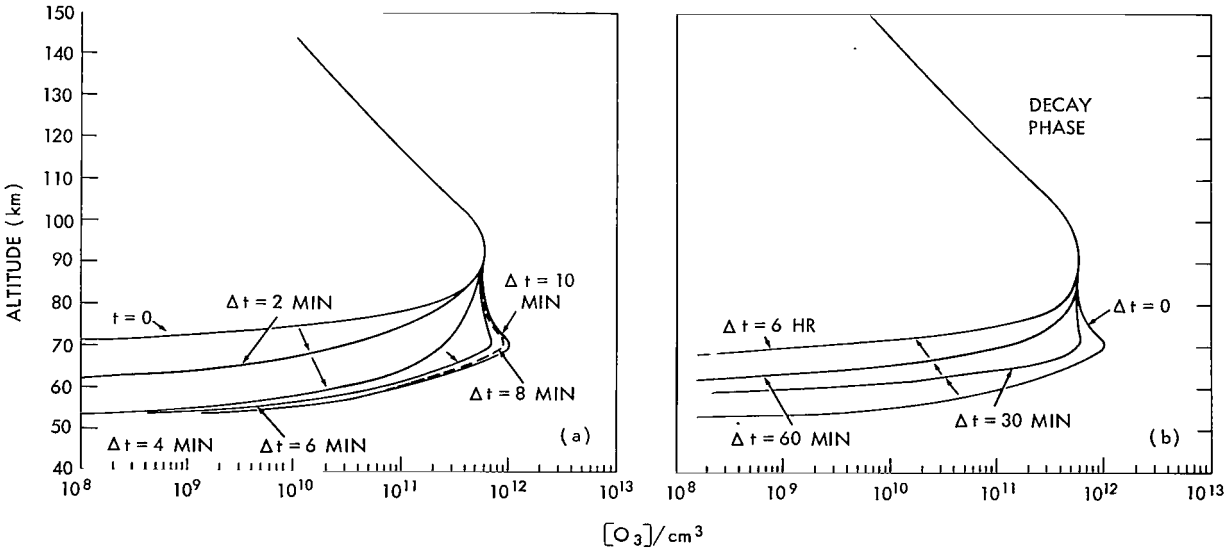

(a) During electron precipitation (increasing phase).

(b) After the cessation precipitation of $J_3 = J_3 \times 10^2$ and $i_0 = 10^{11}$ cm^{-2} sec^{-1}.

Figure 19—Variation of the vertical distribution of atomic oxygen due to the hard spectrum electron precipitation.

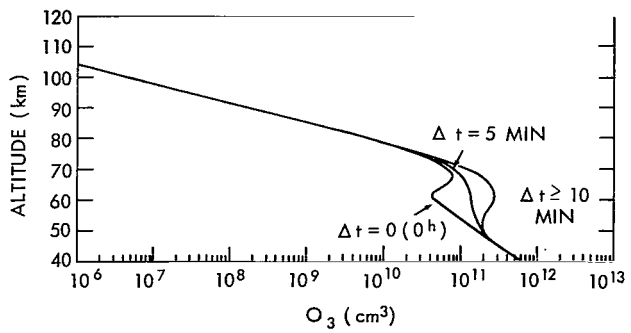

Figure 20—Variation of the vertical distribution of ionospheric ozone during and after hard spectrum electron precipitation for $J_3 = J_2 \times 10^2$ and $i_0 = 10^{11}$ cm^{-2} sec^{-1}.

soft and rather monoenergetic with an energy range of 10 to 50 kev. For events of this type, there is no modification of the atmosphere unless the event is of such a long duration as to increase the atomic oxygen concentration above 90 km. Therefore, significant enhancement of mesospheric ozone during auroral activity (Murcray 1957) seems very unlikely in general, although it may occur for special events. Most of the UV emissions from excited nitrogen molecules originating from auroral electron bombardments are in the far ultraviolet regions which exceed the ionization threshold of molecular oxygen. Therefore, the auroral UV emissions lead to O_2-ionization rather than O_2-dissociation (Green and Barth 1965) and will not affect present results.

Goddard Space Flight Center
National Aeronautics and Space Administration
Greenbelt, Maryland, March 29, 1967
188-46-01-02-51

REFERENCES

Aikin, A. C., "A Preliminary Study of Sunrise Effects in the D Region" in *"Electron Density Profiles in the Ionosphere and Exosphere,"* Ed. B. Maehlum, Pergamon Press, 1962.

Aikin, A. C. and Maier, E., "The Effect of Auroral Bremsstrahlung in the Lower Ionosphere," GSFC Document X-615-63-114, April 1963.

Akasofu, S. I., "A Source of the Energy for Geomagnetic Storms and Auroras," *Planet Space Sci.* 12:801-833, 1964.

Bailey, D. K., Pomerantz, M. A., Sullivan, K. W. and Taib, C. C., "Characteristics of Precipitated Electrons Inferred from Ionospheric Forward Scatter," *J. Geophys. Res.* 71:5179-5182, 1966.

Barth, C. A., "Nitrogen and Oxygen Atomic Reactions in the Chemosphere," in *"Chemical Reactions in the Lower and Upper Atmosphere,"* New York: Interscience Publishers, 1961.

Bates, D. and Nicolet, M., "The Photochemistry of Atmospheric Water Vapor," *J. Geophys. Res.* 55:301-327, 1950.

Bauer, E. and Bartky, C. E., "Calculation of Inelastic Electron-Atom and Electron-Molecule Collision Cross Sections by Classical Methods," Aeronutronic Publication No. U-2943, Philco Corporation, 1965.

Benson, S. W. and Axworthy, A. E., "Reconsideration of the Rate Constants From the Thermal Decomposition of Ozone," *J. Chem. Phys.* 42:2614-2615, 1965.

Brown, R. R., "Feature of the Auroral Electron Energy Spectrum Inferred from Observations of Ionosphere Absorption," *Arkiv, Geofys.* 4:405-426, 1964.

Brown, R. R., "Electron Precipitation in the Auroral Zone," *Space Science Reviews,* 5:311-387, 1966.

Chamberlain, J. W., *"Physics of the Aurora and Airglow,"* New York: Academic Press Inc., 1961.

Chapman, S., "On Ozone and Atomic Oxygen in the Upper Atmosphere," *Phil. Mag.* 10:369-383, 1930.

Colegrove, F. D., Hanson, W. B. and Johnson, F. S., "Eddy Diffusion and Oxygen Transport in the Lower Thermosphere," *J. Geophys. Res.* 70:4931-4941, 1965.

CIRA 1965, (Cospar International Reference Atmosphere 1965, Compiled by the members of COSPAR working group IV), Amsterdam: North-Holland Pub. Co., 1965.

Ditchburn, R. W. and Young, P. A., "The Absorption of Molecular Oxygen between 1850 and 2500 A," *J. Atm. Terr. Phys.* 24:127-139, 1962.

Dütsch, H. U., "Current Problems of the Photochemical Theory of Atmospheric Ozone," *"Chemical Reactions in the Lower and Upper Atmosphere,"* New York: Interscience Pub., 1961.

Fehsenfeld, F. C., Ferguson, E. E. and Schmeltekopf, A. L., "Thermal Energy Association Detachment Reactions of Negative Ions," *J. Chem, Phys.* 45:1844-1845, 1966.

Frost, D. C. and McDowell, C. A., "The Ionization and Dissociation of Oxygen by Electron Impact," *J. Am. Chem. Soc.* 80:6183-6187, 1958.

Gilmore, F. R., "Potential Energy Curves for N_2, NO, O_2, and Corresponding Ions," Rand Corporation Memorandum, RM-4034-PR, June 1964.

Glockler, G. and Wilson, J. L., "The Activation of Molecular Oxygen by Electron Impact," *J. Am. Chem. Soc.* 54(12):4544-4558, 1932.

Golomb, D., Rosenberg, N. W., Aharonian, C., Hill, J. A. F. and Alden, H. L., "Oxygen Atom Determination in the Upper Atmosphere by Chem-Illuminescence of Nitric Oxide," *J. Geophys. Res.* 70:1155-1173, 1965.

Green, A. E. S. and Barth, C. A., "Calculations of Ultraviolet Molecular Nitrogen Emission from the Aurora," *J. Geophys. Res.* 70:1083-1092, 1965.

Grün, A. E., "Lumineszenz-Photometrische Messungen der Energieabsorption im Strahlungsfeld von Elektronenquellen Eindimensionaler Fall in Luft," *Zeit. Naturf,* 12A:89-95, 1957.

Gryzinski, M., "Classical Theory of Electronic and Ionic Inelastic Collisions," *Phys. Rev.* 115:374-383, 1959.

Hesstvedt, E., "On the Determination of Characteristic Times in a Pure Oxygen Atmosphere," *Tellus,* 15:82-88, 1963.

Hinteregger, H. E., "Absolute Intensity Measurements in the Extreme Ultraviolet Spectrum of Solar Radiation," *Space Sci. Rev.* 4:461-497, 1965.

Horiuchi, G., "Odd Oxygen in the Mesosphere and Some Meteorological and Considerations," *Geophys. Mag.* 30(3):439-520, March 1961.

Hultqvist, B., "Aurora," GSFC Document X-611-64-97, April 1964.

Hunt, B. G., "A Non-Equilibrium Investigation into the Diurnal Photochemical Atomic Oxygen and Ozone Variations in the Mesosphere," Technical Note (Australian Weapons Research Establishment) PAD 82, February 1964.

Hunt, B. G., "Influence of Metastable Oxygen Molecules on Atmospheric Ozone," *J. Geophys. Res.* 70:4990-4991, 1965.

Hunt, B. G., "The Need for a Modified Photochemical Theory of the Ozonosphere," *J. Atmos. Soc.* 23:88-95, 1966 a.

Hunt, B. G., "Photochemistry of Ozone in a Moist Atmosphere," *J. Geophys. Res.* 71:1385-1398, 1966 b.

Johnson, F. S., Purcell, J. D. and Tousey, R., "Studies of the Ozone Layer over New Mexico" in "Rocket Exploration of the Upper Atmosphere," Edited by R. Boyd and M. J. Seaton, London: Pergamon Press, 189, 1954.

Johnson, F. S. and Wilkins, E. M., Correction to "Thermal Upper Limit on Eddy Diffusion in the Mesosphere and Lower Thermosphere, *J. Geophys. Res.* 70:4063, 1965.

Kellogg, W. W., "Chemical Heating above the Polar Mesosphere in Winter," *J. Meteorol.* 18:373-381, 1961.

Kellogg, W. W. and Schilling, G. F., "A Proposed Model of the Circulation in the Upper Stratosphere," *J. Meteorol.* 8:222-230, 1951.

Lassettre, E. N., "Collision Cross Section Studies on Molecular Gases and the Dissociation of Oxygen and Water," *Radiation Research, Supplement,* 1:530-546, 1959.

Lassettre, E. N., Silverman, S. M. and Krasnow, M. E., "Electronic Collision Cross Sections and Oscillator Strengths for Oxygen in the Schumann-Range Region," *J. Chem. Phys.* 40:1261-1265, 1964.

Leovy, C., "Radiative Equilibrium of the Mesosphere," *J. Atmos. Sci.* 21:238-248, 1964.

Maeda, K., "On the Heating of the Polar Upper Atmosphere," NASA Tech. Rept. R-141, 1962.

Maeda, K., "Auroral Dissociation of Molecular Oxygen in the Polar Mesosphere," *J. Geophys. Res.* 68:185-197, 1963 a.

Maeda, K., "Diffusion of Low Energy Auroral Electrons in the Atmosphere," *J. Atm. and Terr. Phys.* 27:259-275, 1965 a.

Maeda, K., "Diffusion of Auroral Electrons in the Atmosphere," NASA Technical Note D-2612, February 1965 b.

Maeda, K. and Singer, S. F., "Energy Dissipation of Spiraling Particles in the Polar Atmosphere," *Arkiv, Geophys.* 3:531-538, 1961.

Mann, L. G., Bloom, S. D. and West, Jr., H. I., "The Electron Spectrum from 90 to 1200 kev as Observed on Discoverer Satellites 29 and 31," in *"Space Research III,"* Amsterdam: North-Holland Pub. Co., 447-462, 1963.

Mange, P., "The Diffusion and Dissociation of Molecular Oxygen in the Atmosphere above 100 Km," Scientific Report No. 64, Pennsylvania State Univ., 1954.

Massey, H. S. W., "Negative Ions," London: Cambridge University Press, 1950.

Massey, H. S. W. and Burhop, E. H. S., "Electronic and Ionic Impact Phenomena," London: The Oxford University Press, 1956.

McGowan, J. W., Clark, E. M., Hanson, H. P. and Stebbings, R. F., *Phys. Ref. Letters*, 13:620, 1964.

McIlwain, C. E., "Direct Measurement of Particles Producing Visible Auroras," *J. Geophys. Res.* 65:2727-2747, 1960.

Mikirov, A. Y., "The Estimation of Ozone Concentration at the Heights of 44-102 km during Night Launches of Geophysical Rockets," *Geomag. Aeronom.* 5:1120-1123, 1965 (NASA TT F-10, 006, July 1965).

Mozer, F. S. and Bruston, J. P., "Properties of the Auroral-Zone Electron Source Deduced from Electron Spectrums and Angular Distribution," *J. Geophys. Res.* 71:4451-4460, 1966.

Murcray, W. B., "A Possible Auroral Enhancement of Infra-Red Radiation Emitted by Atmospheric Ozone," *Nature* 180:139-140, 1957.

Nicolet, M., "Aeronomic Conditions in the Mesosphere and Lower Thermosphere," Sci. Rept. April No. 102, 1958.

O'Brien, B. J., "High-Latitude Geophysical Studies with Satellite Injun 3," *J. Geophys. Res.* 69:13-43, 1964.

Rapp, D. and Briglia, D. D., "Total Cross Sections for Negative Ion Formation in Gases by Electron Impact," Lockheed Missile and Space Co., Tech. Rept. 6-74-64-40, 1964.

Rapp, D., Sharp, T. E. and Briglia, D. D., "On the Theoretical Interpretation of Resonance Dissociative Attachment Cross Sections," Lockheed Missile and Space Co., Tech. Rept., 6-74-64-45, 1964.

Rawcliffe, R. D., Meloy, G. E., Friedman, R. M. and Rogers, E. H., "Measurement of Vertical Distribution of Ozone from a Polar Orbiting Satellite," *J. Geophys. Res.* 68:6425-6429, 1963.

Reed, Edith and Scolnik, Reuben, "A Nighttime Measurement of Ozone above 40 km," GSFC Document X-613-64-267, 1964. (Presented in Intn'l. Ozone Symposium, Albuquerque, New Mexico, Sept. 1964.)

Rees, M. H., "Auroral Ionization and Excitation by Incident Energies Electrons," *Planet. Space Science,* 11:1209-1218, 1963.

Reid, G. C., "Physical Process in the D-Region of the Ionosphere," *Review of Geophys.* 2:311-333, 1964.

Reid, G. C., "Physics of the D-Region at High Latitudes," in *"Electron Density Profiles in the Ionosphere and Exosphere,"* Amsterdam: North-Holland Publishing Co., 1966.

Rossi, B., *"High Energy Particles,"* New York: Prentice Hall Inc., 1952.

Schulz, G. J. and Dowell, J. T., "Excitation of Vibrational and Electronic Levels in O_2 by Electron Impact," *Phys. Rev.* 128:114-177, 1962.

Shimazaki, T., "Dynamic Effects on Atomic and Molecular Oxygen Density Distribution in the Upper Atmosphere: A Numerical Solution to Equations of Motion and Continuity," *J. Atm. and Terr. Phys.* 29:723-747, 1967.

Silverman, S. M. and Lassettre, E. N., "Collision Cross Sections for Oxygen in the Excitation Energy Range 10 to 80 V," *J. Chem. Phys.* 40:2922-2932, 1964.

Spencer, L. V., "Energy Dissipation by Fast Electrons," *N.B.S.* Monograph 1:1959.

Tate, J. T. and Smith, P. T., "The Efficiencies of Ionization and Ionization Potential of Various Gases Under Electron Impact, *Phys. Rev.* 39:270-273, 1932.

Wallace, L., "The OH Nightglow Emission," *J. Atmos. Sci.* 19:1-16, 1962.

Watanabe, K., Inn, E. C. Y. and Zelikoff, M., "Absorption Coefficients of Oxygen in the Vacuum Ultraviolet," *J. Chem. Phys.* 21:1026-1030, 1953.

Whitten, R. C. and Poppoff, I. G., "Associated Detachment in the D-Region, *J. Geophys. Res.* 67: 1183, 1962.

Wu, C. S., "The Interaction of Beta Particles with Matter," in "Nuclear Spectroscopy, Part A," Ed. F. Ajzenberg-Selove, New York: Academic Press, 1960.

Young, C. and Epstein, E. S., "Atomic Oxygen in the Polar Winter Hemisphere," *J. Atm. Sci.* 19: 435-443, 1962.

Appendix A

Effects of Diffusion

The diffusion of neutral atoms and molecules in the upper atmosphere can be described in terms of molecular diffusion and eddy diffusion, both of which depend on the vertical gradients of densities, pressures, and temperatures in the atmosphere. Calculations on these effects have been made by several investigators (Mange 1954; Colegrove et al., 1965; Shimazaki, 1966). Numerical computations which include these effects are not impossible, but they create additional complications and increase machine time. Before including such processes, the effects of diffusion can be estimated. Since the products of O_2-dissociation have a finite lifetime in the atmosphere, which changes with altitude, one can define the effective diffusion length of these elements by

$$\ell_i(z) = \left[D_i(z) \cdot \tau_i(z)\right]^{1/2} ,$$

where

$D_i(z)$'s are the diffusion coefficients for O_i at the altitude z km, in $cm^2\ sec^{-1}$, and

$\tau_i(z)$'s are the lifetime of O_i in the atmosphere at the altitude z km, in second, which are shown in Figure 15.

It is known that above a certain altitude (turbopause), the molecular diffusion coefficient exceeds the eddy diffusion coefficient and increases further with altitude. Since the present calculation is an order of magnitude estimation, $D_i(z)$'s are taken from the corrected value given by Johnson and Wilkinson (1965). If $\ell_i(z)$ is less than the local vertical scale for gradient $h_i(z)$ of the element O_i at z in km, the effects of diffusion can be regarded as unimportant; while if $\ell_i(z)$ exceeds $h_i(z)$, diffusion is important to consider in finding the vertical distribution of elements O_i in the atmosphere around the altitude z. The results are shown in Table A1. From this table, we can conclude that the diffusion is not important to determine the vertical distributions of atomic oxygen and ozone below 90 km but cannot be disregarded above the 100-km level. As can be seen from Figure 15, the effect of diffusion is not as important for the ozone distribution as for that of atomic oxygen.

Table A1

The Effective Diffusion Length, ℓ_i (km) and the Local Vertical Scale for Gradient, h_i (in km) in the Mesosphere, Where Suffix i = 1, 3 stand for Atomic Oxygen and Ozone, Respectively.

Altitude z in km	ℓ_1 (oxygen atom)	h_1 (oxygen atom)	ℓ_3 (ozone)	h_3 (ozone)
50	0.06	1	0.22	5.0
60	0.1	3	0.50	6.5
70	0.35	6	0.27	5.0
80	1.8	12	0.18	4.5
90	8.7	21	0.08	4.0
100	120	∞	0.054	3.5
110	3600	13	0.036	3.0
120	$>10^5$	20	0.020	3.0

Appendix B

Analytic Formula for $i(E, E_0, x)$

The number of electrons whose energy is between E and E + dE (in kev) at the atmospheric depth x (g/cm^2), corresponding to monoenergetic vertically incident electrons with energy E_0, $i(E, E_0, x)$ has been calculated by means of the Monte Carlo method (Maeda, 1965). This can be approximated by

$$i(E, E_0, x) = \frac{Ae^{-a(\xi+\xi_0)^b}}{N(E_0, x)} i_0(E, E_0, x) \quad , \tag{B1}$$

where

$$a = 4.42, \qquad b = 2.8, \qquad A = 1, \qquad \xi_0 = 0,$$

and

$$i_0(E, E_0, x) = E_0^{n(\xi)-1} \left[\frac{(1-y)}{(1-y_m)^{0.1}}\right]^{n(\xi)} \exp\left\{-\left[\frac{1-y}{(1-y_m)^{0.9}}\right]^{n(\xi)}\right\} \quad ,$$

$$\xi = x/r_0 , \qquad y = E/E_0 , \qquad y_m = E_m/E_0 , \tag{B2}$$

$$r_0 = 4.57 \cdot 10^{-6} E_0^{7/4} \quad , \tag{B3}$$

$$E_m = \left[(r_0 - x)/r_0\right]^{4/7} \quad , \tag{B4}$$

and

$$N(E_0, x) = \int_0^{E_0} i_0(E, E_0, x)\, dE$$

$$= E_0 \int_0^1 i_0(y, 1, x)\, dy \quad .$$

The empirical formula for a range r_0 (g/cm^2) of electrons with initial energy E_0 (kev) in air shown by Equation B3 (Grün, 1957) and E_m given by Equation B4 corresponds to the residual energy of electrons at the depth x in air.

Since the integrand $i(y, 1, x)$ is independent of E_0, the normalization factor of Equation B1, $N(E_0, x)$, is written as:

$$N(E_0, x) = E_0 \int_0^1 i_0 (y, x)\, dy \quad , \tag{B5}$$

where

$$i_0 (y, x) = \left[\frac{(1-y)}{(1-y_m)^{0.1}}\right]^{n(\xi)} \exp\left[-\left(\frac{1-y}{(1-y_m)^{0.9}}\right)^{n(\xi)}\right] . \tag{B6}$$

Numerical values of Equation B6 for E_0 = 20 kev are shown in Figure 6, with comparison to Monte Carlo results (Maeda, 1965 a,b).

Another term in Equation B1, $Ae^{-(\xi+\xi_0)^b}$, is an empirical expression of total intensity of vertically incident monoenergetic electron E_0, at the depth $x = \xi \cdot r_0$, which also has been computed by the Monte Carlo method (Maeda, 1965). Comparisons of numerical values of this factor and Monte Carlo results are shown in Figure 7.

Appendix C

Integration of the Differential Equations by Finite Difference Method

The differential equation (Equation 11) can be replaced with the following finite difference scheme;

$$\dot{O}_3 \simeq \frac{O_3^{(n+1)} - O_3^{(n)}}{\Delta t} = O_1^{(n)} \left[k_{12} \cdot M \cdot O_2^{(n+1)} - k_{13} \cdot O_3^{(n+1)}\right] - J_3 \cdot O_3^{(n+1)} \quad , \tag{C1}$$

where O_i, $\dot{O}_i$ stand for $[O_i]$ and $d[O_i]/dt$ in Equation 11, and the superscripts n, $n+1$ refer to the time t_n and $t_{n+1} = t_n + \Delta t$, respectively.

Similarly, Equation 12 can be replaced by

$$\dot{O}_1 \simeq \frac{O_1^{(n+1)} - O_1^{(n)}}{\Delta t} = 2J_2 \cdot O_2^{(n+1)} + J_3 \cdot O_3^{(n+1)} + O_1^{(n)} \left[-2k_{11} \cdot M \cdot O_1^{(n+1)} - k_{12} \cdot M \cdot O_2^{(n+1)} - k_{13} \cdot O_3^{(n+1)}\right] \quad . \tag{C2}$$

Corresponding to the reactions listed in Table 2, time variation of O_2 also can be written as;

$$\dot{O}_2 \simeq \frac{O_2^{(n+1)} - O_2^{(n)}}{\Delta t} = O_1^{(n)} \left[k_{11} M \cdot O_1^{(n+1)} + 2k_{13} O_3^{(n+1)}\right] - O_2^{(n+1)} \cdot \left[k_{12} M \cdot O_1^{(n+1)} + J_2\right] + J_3 \cdot O_3^{(n+1)} \tag{C3}$$

This equation can be also derived by Equations 11 and 12 with a condition for conservation of oxygen allotrope at each layer; i.e.,

$$3[O_3] + 2[O_2] + [O_1] = \text{const.}$$

or

$$\dot{O}_2 = \frac{-1}{2} \left[\dot{O}_1 + 3\dot{O}_3\right] \quad . \tag{C4}$$

It should be noted that Equations C1, C2, and C3 are written in linear form which can be simplified by writing in matrix, i.e.,

$$\begin{pmatrix} O_1^{(n)} \\ O_2^{(n)} \\ O_3^{(n)} \end{pmatrix} = \begin{pmatrix} 1 + O_1^{(n)} \cdot 2k_{11} M\Delta t & \left(O_1^{(n)} k_{12} M - 2J_2\right)\Delta t & \left(O_1^{(n)} k_{13} - J_3\right)\Delta t \\ -O_1^{(n)} k_{11} M\Delta t & 1 + \left(O_1^{(n)} k_{12} M + J_2\right)\Delta t & -\left(O_1^{(n)} 2k_{13} + J_3\right)\Delta t \\ 0 & -O_1^{(n)} k_{12} M\Delta t & 1 + \left(O_1^{(n)} k_{13} + J_3\right)\Delta t \end{pmatrix} \begin{pmatrix} O_1^{(n+1)} \\ O_2^{(n+1)} \\ O_3^{(n+1)} \end{pmatrix}.$$

By means of matrix inversion $O_i^{(n+1)}$'s are easily obtained by knowing $O_i^{(n)}$'s, starting from certain initial conditions. As can be seen from Equations C1 and C3, replacement of original differential Equations 11 and 12 by the finite difference schemes is not unique. It should be noted, however, that partial replacements such as $O_i^{(n+1)} \cdot O_i^{(n+1)}$ by $O_i^{(n)} \cdot O_i^{(n+1)}$ are essential to retain the linearity of the scheme by which integration stability in numerical integrations is to be achieved easily.

The present method works for $\Delta t = 20$ sec for altitudes of 50 to 150 km and seems progressively unstable below 50 km for $\Delta t = 20$ sec, which can be extended, however, by reducing Δt.

"The aeronautical and space activities of the United States shall be conducted so as to contribute . . . to the expansion of human knowledge of phenomena in the atmosphere and space. The Administration shall provide for the widest practicable and appropriate dissemination of information concerning its activities and the results thereof."

—NATIONAL AERONAUTICS AND SPACE ACT OF 1958

NASA SCIENTIFIC AND TECHNICAL PUBLICATIONS

TECHNICAL REPORTS: Scientific and technical information considered important, complete, and a lasting contribution to existing knowledge.

TECHNICAL NOTES: Information less broad in scope but nevertheless of importance as a contribution to existing knowledge.

TECHNICAL MEMORANDUMS: Information receiving limited distribution because of preliminary data, security classification, or other reasons.

CONTRACTOR REPORTS: Scientific and technical information generated under a NASA contract or grant and considered an important contribution to existing knowledge.

TECHNICAL TRANSLATIONS: Information published in a foreign language considered to merit NASA distribution in English.

SPECIAL PUBLICATIONS: Information derived from or of value to NASA activities. Publications include conference proceedings, monographs, data compilations, handbooks, sourcebooks, and special bibliographies.

TECHNOLOGY UTILIZATION PUBLICATIONS: Information on technology used by NASA that may be of particular interest in commercial and other non-aerospace applications. Publications include Tech Briefs, Technology Utilization Reports and Notes, and Technology Surveys.

Details on the availability of these publications may be obtained from:

SCIENTIFIC AND TECHNICAL INFORMATION DIVISION

NATIONAL AERONAUTICS AND SPACE ADMINISTRATION

Washington, D.C. 20546